Disentangling Cro-Magnon: The Pedal Remains

Erik Trinkaus, Adrien Thibeault, Sébastien Villotte

Disentangling Cro-Magnon: The Pedal Remains

Erik Trinkaus,[a,b,c,*] Adrien Thibeault[d] and Sébastien Villotte[d,e]

[a] Department of Anthropology, Washington University, Saint Louis, MO 63130, USA;
trinkaus@wustl.edu

[b] 32 Cliff Street, Burlington, VT 05401, USA

[c] Department of Anthropology, University of Vermont, Burlington, VT 05405, USA

[d] Université de Bordeaux, CNRS, PACEA, UMR 5199, F-33615 Pessac, France;
adrien.thibeault@u-bordeaux.fr; sebastien.villotte@u-bordeaux.fr

[e] Operational Directory Earth and History of Life, Royal Belgian Institute of Natural Sciences, Brussels, Belgium

* Corresponding author

The authors declare no conflicts of interest.

Author contributions:
Erik Trinkaus: Conceptualization, Data curation, Investigation, Methodology, Visualization, Writing - original draft. **Adrien Thibeault**: Methodology, Visualization, Writing-review & editing. **Sébastien Villotte**: Conceptualization, Funding acquisition, Investigation, Project administration, Resources, Writing - original draft.

Corresponding author: Erik Trinkaus
trinkaus@wustl.edu
32 Cliff Street, Burlington ,VT 05401, USA

Highlights

- The Cro-Magnon human remains include 17 pedal bones, including 9 tarsals, 7 metatarsals and a phalanx.
- The pedal remains can be grouped into three individuals, corresponding to the Alpha, Beta and Gamma Cro-Magnon postcranial individuals.
- The pedal length proportions and articular morphology are unexceptional for Late Pleistocene and recent humans.
- The Beta and especially the Gamma tali provide evidence of habitual talocrural dorsiflexion (squatting).
- The Alpha first metatarsophalangeal articulations indicate normal hallucal orientation.
- The Alpha distal metatarsals 4 and 5 and hallucal phalanx provide further manifestations of the systemic abnormalities of Cro-Magnon 1.

Abstract

The seventeen human pedal remains from Cro-Magnon (2 tali, 7 subtalar tarsals, 7 metatarsals, and a proximal phalanx) can be grouped into three individual sets of bones, based on articular congruence, symmetry, size, and pathology. They correspond to the previously identified (Thibeault and Villotte, J. Arch. Sci. Rep. 21, 76-86, 2018) Alpha (Cro-Magnon 1), Beta and Gamma postcranial individuals. The Alpha and Gamma pedal remains are of average size for the Mid Upper Paleolithic, whereas the Beta talus is relatively small. The Gamma pedal length proportions are similar to other Late Pleistocene and recent humans, including foot length to femur length. The tarsal articulations are unexceptional for Late Pleistocene and recent humans, notable only for the evidence for habitual talocrural dorsiflexion, as is indicated by distal trochlear extensions, a squatting facet and large sulcus tali facets. The Alpha first metatarsophalangeal articulations indicate normal hallucal orientation. The Alpha metatarsals 4 and 5 and hallucal phalanx distal pathological alterations provide further evidence of the Cro-Magnon 1 systemic abnormalities.

Key Words: Paleoanthropology, Upper Paleolithic, Feet, Talus, Hallux, Paleopathology

1. Introduction

The Cro-Magnon rock shelter (Les Eyzies-de-Tayac-Sireuil, Dordogne, France) is one of the premier Upper Paleolithic sites, best known for establishing in 1868 the contemporaneity of early modern humans with Upper Paleolithic assemblages and Pleistocene fauna (Broca, 1868; Lartet, 1868). Although described in variable detail by Broca (1868) and Pruner-Bey (1865-75), and reassessed 100 years later by Vallois and Billy (1965) and Dastugue (1967), the human skeletal assemblage from Cro-Magnon has remained poorly known despite the incorporation of data from it into Late Pleistocene comparative analyses. In this context, and in the framework of a broader refocus on western Eurasian Upper Paleolithic human paleobiology, we have undertaken the reassessment of the Cro-Magnon human remains (Thibeault and Villotte, 2018; Villotte and Balzeau, 2018; Partiot et al., 2020; Villotte et al., 2020; Trinkaus et al., 2021).

The relatively abundant human remains represent all portions of the skeleton. However, they became commingled, whether in situ or subsequently, resulting in various attempts to re-associate them by individual (e.g., Broca, 1868; Pruner-Bey, 1865-75; Vallois and Billy, 1965; Henry-Gambier et al., 2013; Thibeault and Villotte, 2018; Villotte and Balzeau, 2018; Villotte et al., 2020; Trinkaus et al., 2021). Based on the craniofacial and upper limb remains, four adults are present (Broca, 1868; Lartet, 1868; Pruner-Bey, 1865-75; Vallois and Billy, 1965; Villotte et al., 2020; Trinkaus et al., 2021), although only three are evident in the pelvic and leg remains (Thibeault and Villotte, 2018). The four adult postcranial individuals are designated Alpha to Delta (Villotte et al., 2020), given the uncertain associations of Beta to Delta with the numbered craniofacial remains (Trinkaus et al., 2021). Alpha, Beta and Gamma older adults are pelvically sexed as male, female and male respectively (Gambier et al., 2006; Thibeault and Villotte, 2018); the age and sex of Delta are unknown.

In this contribution to the reassessment of the Cro-Magnon assemblage, we focus on the pedal remains, seventeen bones which have only been partially sorted and/or analyzed in the past (e.g., Pruner-Bey, 1865-75; Vallois and Billy, 1965; Dastugue, 1967; Thibeault and Villotte, 2018).

2. Materials and Methods

2.1 The Cro-Magnon Pedal Remains

The human remains from the Abri de Cro-Magnon are curated in the Musée de l'Homme, Muséum national d'Histoire naturelle (MNHN), Paris. The specimens of consideration here consist of nine complete tarsals (Cro-Magnon [CM] 4336 to 4344), six complete metatarsals (CM 4345 to CM 4349), one partial metatarsal (CM 4350) and a proximal hallucal phalanx (CM 4351). Additional data derive from the associated femoral and tibial remains. Data were collected in the Musée de l'Homme in 1980 (ET), 2008 (SV) and 2018 (SV and ET).

The human remains from Cro-Magnon were formerly attributed to the "Aurignacian" *sensu lato*. They are now dated to an early phase of the Gravettian technocomplex (33–31,000 cal BP), part of the Mid Upper Paleolithic (MUP) (Henry-Gambier, 2002; Henry-Gambier et al., 2013).

2.2 Comparative Samples

A pooled sample of recent human associated pedal skeletons was employed to assess within-foot proportions and hence possible associations of non-articulating pedal bones. They consist of the remains of Native Americans, Euroamericans, Afroamericans, and Europeans (Trinkaus, 1975a; Pablos et al., 2017; Table S15).

In the morphometric assessments of the Cro-Magnon pedal remains, comparisons are made principally to western Eurasian Mid (MUP) and Early (EUP) Upper Paleolithic remains (E/MUP when pooled). Additional data from Late Upper Paleolithic humans (LUP), Middle Paleolithic modern humans (MPMH) and Neandertals provide a broader framework, as do data from pooled recent human samples (as available; Tables S15 and S16). Data are from personal measurement and primary published descriptions of the paleontological remains.

2.3 Methods

The reassessment of these remains is based on the visual observation of the original remains in the Musée de l'Homme in 2018 (ET and SV), combined with measurements taken in 1980 (ET). Microtomodensitometric (µCT) data for these bones were acquired at the AST-RX platform in the MNHN. They were obtained with the microfocus tube of the µCT scanner "v|tome|xL 240" (GE Sensing and Inspection Technologies Phoenix X ray). Two µCT acquisitions were done: one for the tarsals (CM 4336 to 4344) and another for the metatarsals and proximal hallucal phalanx (CM 4345 to 4351). Each final volume was then reconstructed

with isotropic voxels, 73µm for the tarsals and 105 µm for the metatarsals and proximal hallucal phalanx, using NRecon v2.0 (Bruker microCT) in 16-bit format. Surface rendering of these 3D models was obtained with Avizo v.9 (Visualization Sciences Group Inc.).

In order to evaluate the associations of the pedal remains from Cro-Magnon, the 17 bones were combined into partial pedal skeletons based on matching antimeres, articular congruence, proportions within pedal skeletons, and patterns of pathological lesions. The use of symmetry for antimeres is based on the generally low level of asymmetry in the human lower limb (Auerbach and Ruff, 2006) despite some asymmetry in pedal articular facets (Trinkaus, 1978). The assessment of articular congruence was done with the original bones when possible from the same side; otherwise it was done virtually by mirror imaging potentially matching bones and then assessing the articular fit virtually and visually (Figs. S13 to S15). The evaluation of whether non-adjacent tarsals, metatarsals and the hallucal proximal phalanx could derive from the same individual was done by predicting confidence intervals for the tarsal dimension or metatarsal articular length of one from the articular length(s) of the other metatarsal(s), based on the Native American sample (for the navicular; n = 40) or the pooled sample of Native Americans, Euroamericans, Afroamericans and Europeans (for the others; n = 215 to 233) (Table S9).

Osteometrics principally follow the Martin system (Bräuer, 1988), with additional measurements as defined in Trinkaus et al. (2014, 2017). Discrete traits follow Barnett (1954) and Trinkaus (1975a, 1975b). The quantitative comparisons were done using NCSS (2016).

3. Results

3.1 Associations

The pedal remains are associated into three partial pedal skeletons, designated Feet A to Feet C. These associations account comfortably for ten of the pedal remains. Five more bones can be assigned reasonably to Feet A and B, but the last two bones have less secure associations.

3.1.1 Previous Attempts at Associations

There have only been a few, and partial, attempts to associate Cro-Magnon pedal remains with each other and with individuals. Pruner-Bey (1865-75) attributed the right calcaneus (CM 4336) to Cro-Magnon 1, as did Vallois and Billy (1965). The latter suggested that the CM 4337

talus also derived from Cro-Magnon 1, and they noted the "perfect" articulation of the CM 4338 talus with the CM 4339 navicular. They also combined the proximal hallucal phalanx (CM 4351) with the CM 4345 metatarsal 1. More recently, Thibeault and Villotte (2018) mirrored imaged the CM 4336 calcaneus and noted its articulation with the CM 4337 talus, as well the articulation of CM 4337 with the CM 4330 tibia, part of the Gamma appendicular remains.

3.1.2 The Cro-Magnon Feet A

The most complete of the Cro-Magnon pedal skeletons builds from the CM 4337 left talus to the CM 4345 first metatarsal. As documented by Thibeault and Villotte (2018), the CM 4337 left talus forms an excellent articulation virtually with the mirror imaged CM 4336 right calcaneus (Figs. 1 and S13). The mirror imaged CM 4336 calcaneus then forms an appropriate articulation with the CM 4341 left cuboid bone (Figs. 1 and S14). The CM 4341 cuboid bone articulates cleanly with the CM 4343 left lateral cuneiform bone, which forms part of a tightly articulating set of cuneiform bones with the left CM 4342 and CM 4344 medial and intermediate cuneiform bones (Fig. S15).

The CM 4345 left metatarsal 1 (MT-1) is damaged and reconstructed on the lateral half of the base (Figs. 1 and S15). However, the medial half of the articulation, especially the mediodorsal portion of the tarsal facet, articulates well with the CM 4342 medial cuneiform bone.

The five left tarsal bones, plus the mirror imaged calcaneus, thus form a largely complete tarsal skeleton for Feet A. Neither of the two navicular bones fits appropriately with these tarsals. The right CM 4339 navicular bone is too small for the head of the CM 4337 talus, and mirror imaging it would not alleviate the discordance. The right CM 4340 navicular bone is an appropriate size for the CM 4337 talus, but a virtual attempt to match its mirror image to the articulated cuneiform bones failed to produce a congruent articulation. The right CM 4338 talus does not make an appropriate antimere for CM 4337 given size differences (Table S1, Figs. 2 and S1), it does not articulate properly with the CM 4336 calcaneus, and its length (49.2 mm) is outside of the 95% CI predicted from the CM 4345 MT-1 articular length (50.2 – 59.1 mm) (Table S9).

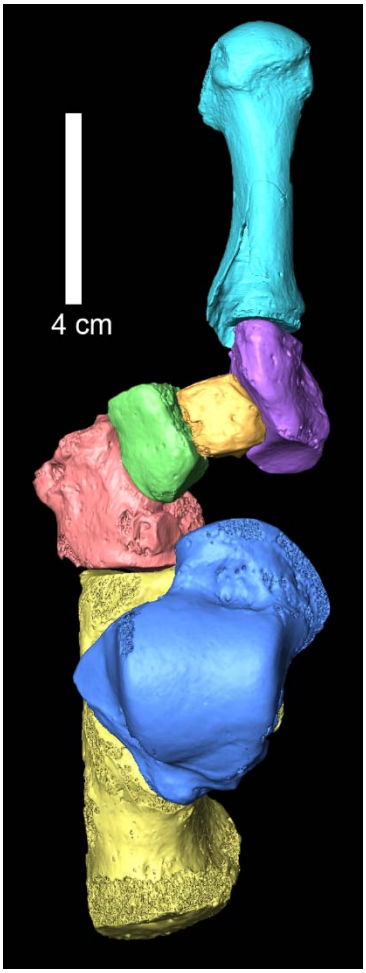

Figure 1. Dorsal view of the virtually articulated left foot of Feet A. It includes the CM 4337 talus, the CM 4336 calcaneus (mirrored), the CM 4341 to CM 4344 cuboid and cuneiform bones, and the CM 4345 metatarsal 1.

These seven bones therefore form an articulation core of Feet A. The CM 4348 left MT-4 does not articulate properly with the CM 4341 left cuboid bone, and by extension (see below) the CM 4347 MT-4 and CM 4349 MT-5 do not belong to Feet A. Similarly, the CM 4350 left MT-5 does not articulate properly with the CM 4341 cuboid bone, and the CM 4345bis right MT-1 does not articulate properly the distal CM 4342 medial cuneiform (even adjusting for side).

It is possible that the CM 4346 right MT-2 belongs to Feet A, even though its tarsal facet breadth (12.3 mm) is smaller than the distal articular breadth of the CM 4344 intermediate cuneiform bone (13.3 mm). Moreover, the 95% CI for the predicted MT-2 articular length from that of the CM 4345 MT-1 (73.2 – 82.5 mm) barely includes the articular length of the CM 4346 MT-2 (74.0 mm) (Table S9).

The remaining bone for Feet A consideration is the CM 4351 hallucal proximal phalanx (PP-1). Its proximal facet articulates well with the head of the CM 4345 MT-1 [as noted by Vallois and Billy (1965)]. The predicted articular length from the CM 4345 articular length (31.8 mm; 95% CI: 28.3 – 35.2 mm) is modestly longer than the articular length of CM 4351 (≈30.5 mm), but its 95% CI comfortably includes the PP-1 length (Table S9). However, the same criteria hold for the CM 4345bis MT-1 (see below).

In addition, as noted above, the CM 4337 talus articulates with the CM 4330 left tibia, which is a portion of the Gamma appendicular skeleton. Feet A therefore become a pedal extension of that postcranial individual. And contra Pruner-Bey (1865-75) and Vallois and Billy (1965), they are not likely to derive from Cro-Magnon 1 (Trinkaus et al., 2021; see below).

3.1.3 The Cro-Magnon Feet B

The second set of articulating Cro-Magnon foot bones consist of the right CM 4347 MT-4 and CM 4349 MT-5. They articulate excellently at the intermetatarsal facet, provide a continuous cuboid articulation, have matching adjacent torsions, and both exhibit pathological alterations of the head. The left CM 4348 MT-4 is an antimere of CM 4347; they have essentially the same maximum lengths (74.2 and 73.9 mm), and they agree in the details of their proximal tarsometatarsal and intermetatarsal facets, diaphyseal curvatures, interosseus muscle markings, and head curvatures [despite head articular changes on CM 4347 (Fig. S10)].

Although its association cannot be confirmed through articulations, the CM 4345bis right MT-1 makes a good match in terms of length with the CM 4347 MT-4 and CM 4349 MT-5. The predicted articular length of the MT-1 from the CM 4347 and CM 4349 right metatarsals (62.6 mm; 95% CI: 57.9 – 67.3 mm) is essentially the same as the articular length of CM 4345bis (62.9 mm) (Table S9).

It is also likely that the CM 4346 right MT-2 is part of the Cro-Magnon Feet B. Its predicted articular length from the CM 4347 and CM 4349 MT-4 and MT-5 is 75.8 mm (95% CI: 71.9 – 79.6 mm), which is slightly larger than its value of 74.0 mm but closer than the value predicted from the Feet A CM 4345 MT-1 (Table S9). The CM 4345bis MT-1 provides a predicted articular length close to that from the MT-4 and MT-5 (75.4 mm; 70.7 – 80.1). In addition, both the CM 4345bis MT-1 and the CM 4346 MT-2 lack evidence of a metatarsal 1-2 articular facet (Figs. S8 and S9).

Given the absence of articulating tarsal bones with the metatarsals of Feet B, it needs to be evaluated whether the CM 4338 right talus could belongs to the same feet. Prediction of talar length from the Feet B metatarsal articular lengths provides a large 95% CI (47.8 – 59.4 mm) that barely includes the length of the CM 4338 talus (49.2 mm). It is therefore possible but unlikely that CM 4338 (and its articulating navicular bone, CM 4339; see below) derive from Feet B.

Assuming that the CM 4338 and CM 4339 talus/navicular are not part of Feet B (see below), it is possible that the CM 4340 right navicular bone derives from Feet B. It is not appropriate for Feet A (see above), and it duplicates CM 4339. Comparisons of its talar facet length (28.7 mm) and breadth (22.0) to those predicted from the Feet B right metatarsal 1, 4 and 5 articular lengths (length: 28.2 mm, 95% CI: 25.0 – 28.7 mm; breadth: 21.1 mm, 95% CI: 18.7 – 23.5 mm) makes its dimensions compatible with the dimensions of Feet B. It is therefore likely, in part by default, that the CM 4340 navicular bone derives from Feet B, rather than the CM 4339 one.

The remaining bone for Feet B consideration is the CM 4351 PP-1. Its proximal facet articulates well with the head of the CM 4345bis MT-1, and the predicted articular length from the CM 4345bis articular length (30.7 mm, 95% CI: 27.3 – 34.1 mm) matches the articular length of CM 4351 (≈30.5 mm) (Table S9). The same criteria hold for the CM 4345 MT-1 (see above), although the length predicted from CM 4345bis matches that of CM 4351 modestly better. Moreover, the head of the CM 4351 PP-1 exhibits the same kinds of articular changes as the CM 4347 and CM 4349 metatarsals.

3.1.4 The Cro-Magnon Feet C

The CM 4338 right talus and the CM 4339 right navicular bone articulate tightly, making them a secure pair [as noted by Vallois and Billy (1965)]. As noted above, the CM 4338 talus does not make an appropriate antimere for CM 4337, and it does not otherwise fit the tarsals of Feet A. It is also unlikely to be a portion of Feet B, given its modest size relative to its metatarsal lengths. CM 4338 and CM 4339 are therefore from a third individual, smaller than those of Feet A and B, and designated Feet C.

The one remaining unassigned pedal element from Cro-Magnon is the CM 4350 left metatarsal 5 (Fig. S11). It does not articulate appropriately with the CM 4341 cuboid bone. It

does not make an appropriate antimere morphologically for the 4349 right metatarsal 5, especially given the high degree of symmetry of the CM 4347 and CM 4348 fourth metatarsals. It is slightly smaller than CM 4349 in most comparable dimensions, as are CM 4338 versus CM 4337 and CM 4339 vs. CM 4340. It is therefore possible that it derives from Feet C.

3.1.5 Associations with Other Cro-Magnon Remains

It is therefore possible, based in articular congruence, bilateral symmetry, recent human pedal bone proportions, and (for the CM 4351 phalanx) shared abnormalities, to group the Cro-Magnon pedal remains into three individuals (Feet, A, B and C) (Table 1). Fifteen of the 17 elements can be attributed to one or the other of these pedal individuals at the secure or probable level. Two of them, however, the CM 4340 navicular bone and the CM 4350 fifth metatarsal, can only be aligned by the defaults of being unlikely or impossible to associate with the other two pedal individuals.

The other lower limb remains, from the sacrum to the malleoli, represent only three individuals (Alpha to Gamma) (Thibeault and Villotte, 2018), although the upper limb remains include a fourth individual (Delta) (Villotte et al., 2020) and four individuals are present in the craniofacial remains (Vallois and Billy, 1965; Trinkaus et al., 2021). Given the presence of only three individuals in the pelvis and leg bones, it is simplest to attribute CM 4340 and CM 4350 to Feet B and C respectively as indicated in Table 1. It nonetheless remains possible that one or both of them represents a fourth individual from Cro-Magnon. If they represent a fourth adult (Delta?), it changes little in the morphological considerations of these pedal remains.

As noted above, the CM 4337 talus (and hence Feet A) articulates appropriately with the CM 4330 tibia, which is part of Gamma. Therefore, the previous referrals of the CM 4336 and 4337 calcaneus and talus to Cro-Magnon 1 (or Alpha) by Pruner-Bey (1865-75) and Vallois and Billy (1965) cannot be maintained. Alpha is a large individual with widespread pathological lesions (Pruner-Bey, 1865-75; Dastugue, 1967; Thibeault and Villotte, 2018), which is associated with the Cro-Magnon 1 cranium and mandible (Trinkaus et al., 2021); given its size and distal metatarsal (plus probably distal phalangeal) articular lesions, it is likely that Feet B is part of Alpha, and hence Cro-Magnon 1. Feet C is smaller than the other two pedal sets, and therefore it is compatible with the smaller Beta postcranial individual. Given that it is unclear which of the Beta to Delta postcranial individuals is associated with which of the Cro-Magnon 2

to 4 craniofacial remains (Trinkaus et al., 2021), their designations should remain either as Feet A to C or Gamma, Alpha (Cro-Magnon 1) and Beta respectively.

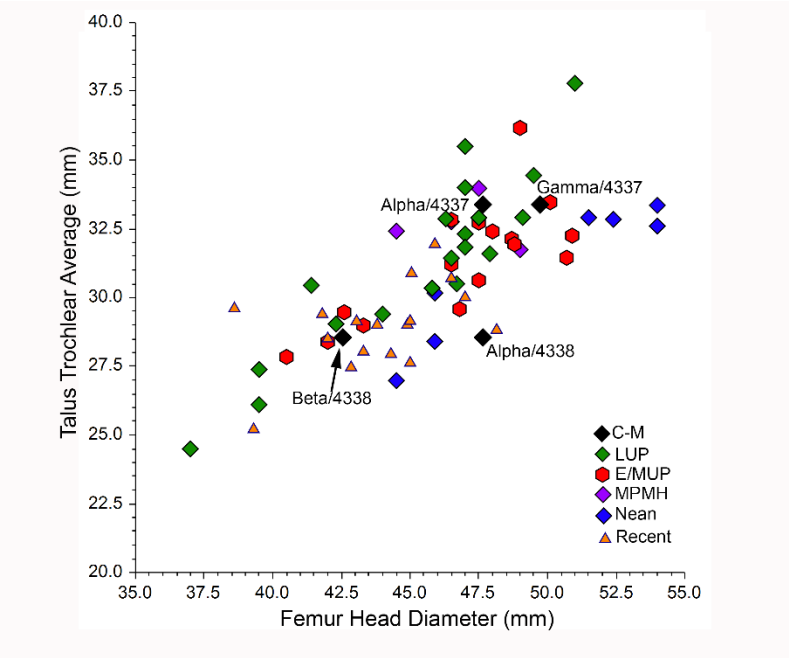

Figure 2. Bivariate distribution of the talar trochlear length and breadth average versus femoral head diameter, for a pooled sample of Late Pleistocene and recent humans. Values of Alpha with CM 4337 (Alpha/4337) and CM 4338 (Alpha/4338), Beta with CM 4338 (Beta/4338) and Gamma with CM 4338 (Gamma/4338) are provided.

Support for these pedal to long bone individual attributions is provided by assessments of talar trochlear size (the trochlear length and breadth average) versus femoral head diameter (Fig. 2; Tables S10 and S11). The bivariate position of the CM 4337 talus versus the Gamma femoral head size is in the middle of the reference distribution, and its trochlear average of 33.4 mm is close to the predicted value of 32.8 mm. Similarly, the bivariate location of the CM 4338 talus versus the Beta femoral head diameter is centered on the reference distribution, and its trochlear average of 28.5 mm is close to the predicted 28.9 mm. The bivariate location of the CM 4337 talus versus the Alpha femoral head size falls close to that for Gamma, but the position of the CM 4338 talus versus Alpha is at the limits of the comparative distribution (Fig. 2). The latter comparison is reinforced by the predicted 95% CI for trochlear size from the Alpha femoral head value (28.3 – 35.1 mm), which would barely include the CM 4338 value. Given the articulation

of CM 4337 with the Gamma CM 4330 tibia, and hence its exclusion from being part of Alpha, these comparisons reinforce the associations of Feet A with Gamma, Feet B with Alpha, and Feet C with Beta. The resultant skeletal elements attributed to each of these Cro-Magnon individuals, Alpha to Delta, are provided in Table S17.

Table 1. Proposed associations of the Cro-Magnon pedal remains by individual. Parentheses around a specimen number indicate uncertainty in its attribution; a question mark indicates additional uncertainty, given assignment in part by default. See Table S12 for the degrees of confidence in the attributions.

Bone	***Feet A***	***Feet B***	***Feet C***
Talus	4337		4338
Calcaneus	4336		
Navicular		(4340?)	4339
Cuboid	4341		
Medial cuneiform	4342		
Intermediate Cuneiform	4344		
Lateral Cuneiform	4343		
Metatarsal 1	4345	4345b	
Metatarsal 2		(4346)	
Metatarsal 4		4347, 4348	
Metatarsal 5		4349	(4350?)
Proximal phalanx 1		(4351)	

3.2 Morphology

3.2.1 Pedal Dimensions and Proportions

The overall size of the Cro-Magnon pedal remains is reflected in the tarsometatarsal (TMT) length of the Feet A/Gamma articulated bones (proximal calcaneus to distal MT-1) and the lengths of the tali and MT-1s (Tables S1, S6 and S13; Figs. 1 and S16). The Feet A TMT length of 190 mm is close to the mean of a small E/MUP sample (186.2 mm, n = 6), similar to the one for Předmostí 3 (192 mm) but below the high value for Pavlov 37 (200 mm). The length of the CM 4337 talus (56.3 mm), as part of Feet A, falls modestly above the average (53.9 ± 4.3 mm, n = 24) of an E/MUP sample, but among the larger of the other Late Pleistocene samples

(Figs. 3 and 4). The CM 4338 talus, however, has a length (49.2 mm) that is substantially smaller, falling only above the values for Dolní Věstonice 3 and Předmostí 9 and similar to the measures for Grotte-des-Enfants 5 and Pataud 1, all females (Fig. 4). The lengths of the CM 4345 (65.2 mm) and 4345bis (62.9 mm) MT-1s, as portions of Feet A and B, fall in the middle of the E/MUP sample (63.9 ± 6.0 mm, n = 16) and among the longer Late Pleistocene ones (Fig. 4). All of these dimensions, and particularly those of Feet A and B, reflect the generally high statures of these E/MUP individuals (Trinkaus, 2006; Holt and Formicola, 2008; see below).

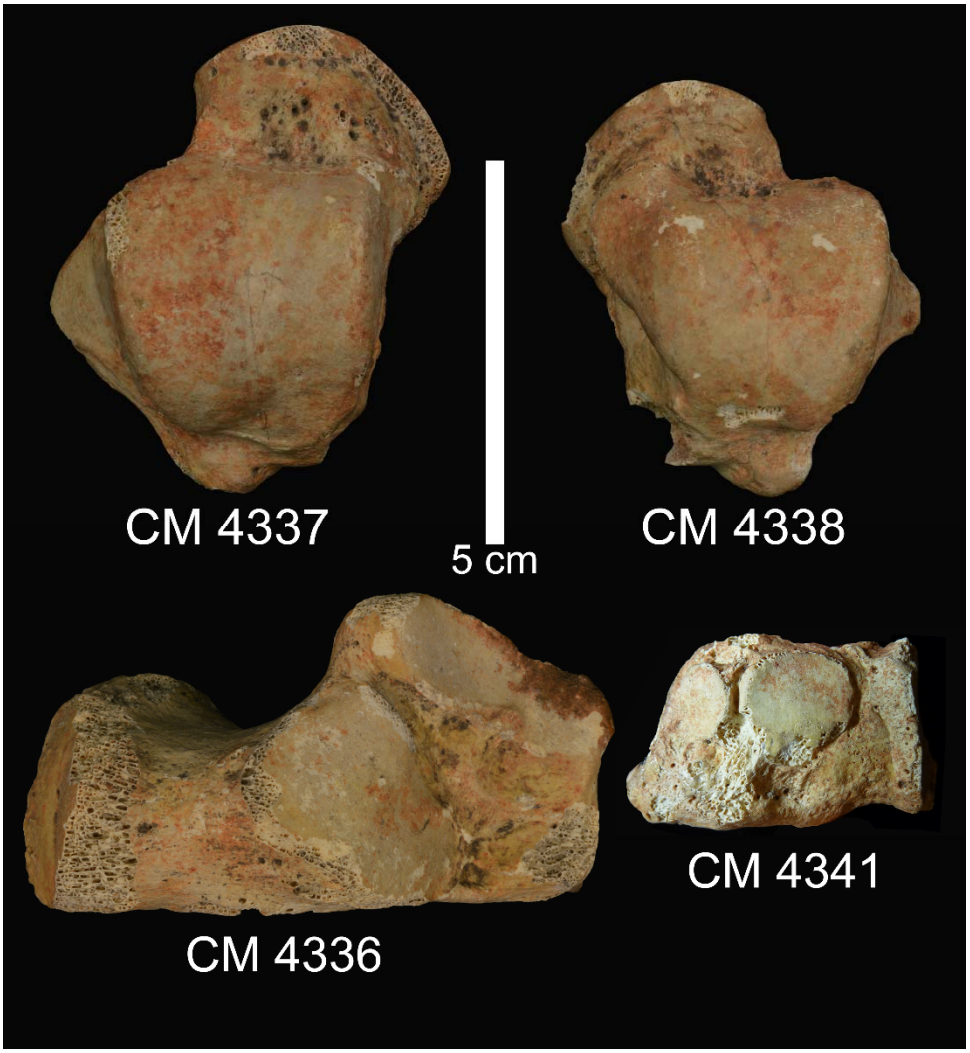

Figure 3. Tarsals from Cro-Magnon, including the CM 4337 and 4338 tali in dorsal view, the CM 4336 calcaneus in dorsal view, and the CM 4341 cuboid bone in medial view.

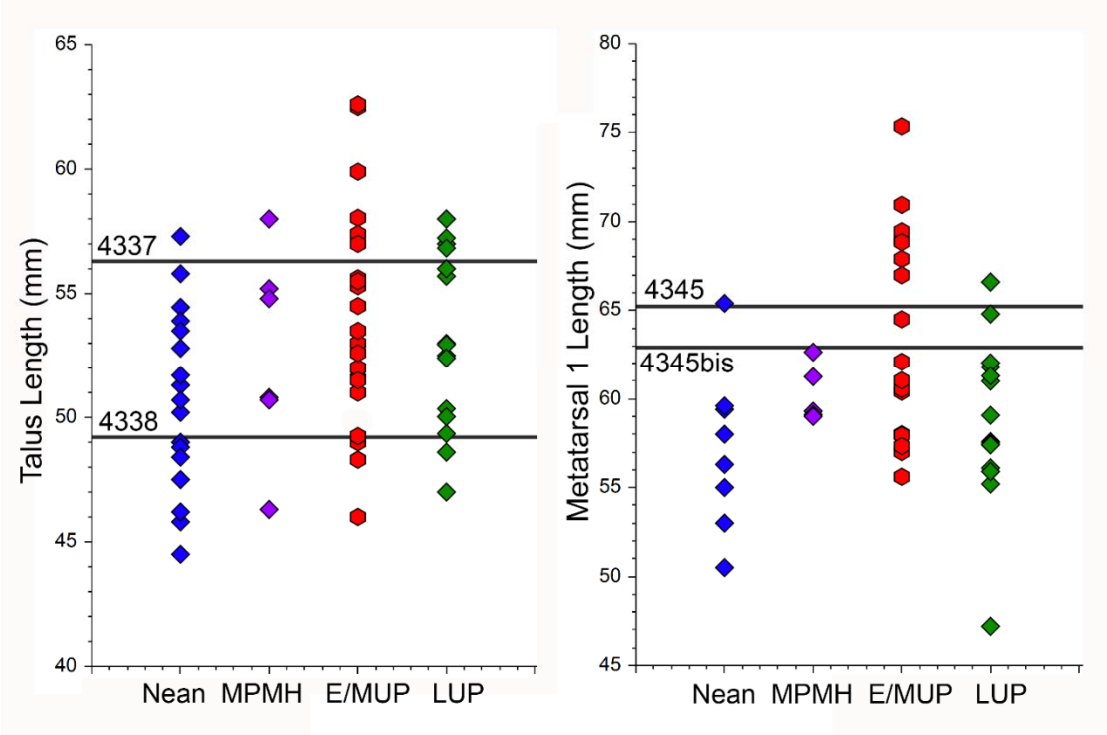

Figure 4. The talus lengths and the metatarsal 1 articular lengths from Cro-Magnon and comparative Late Pleistocene samples. Nean: Neandertals; MPMH: Middle Paleolithic modern humans; E/MUP: Early/Mid Upper Paleolithic; LUP: Late Upper Paleolithic.

Relative foot length can be assessed by comparing the Feet A TMT length to femoral bicondylar length, as an index [using the length of the CM 4322 femur (Thibeault and Villotte, 2018; see Table S13)]. The resultant index for Feet A of 40.0 is close to those of Caviglione 1 (39.9) and Předmostí 3 (39.5) and modestly above those of Sunghir 1 (36.7) and Dolní Věstonice 16 (38.5). None of these values are exceptional relative to a recent human sample (Native Americans and North Africans; 37.4 ± 2.0, n = 40). Therefore, contra Pruner-Bey (1865-75: 84), the Cro-Magnon foot was not "long, compared with the length of the long bones." Similarly, for within-foot proportions, an index of talus to TMT length provides a value of 29.6 for Feet A, which is in the middle of the E/MUP distribution (29.7 ± 1.0, n = 7) and well within a recent human sample's variation (30.2 ± 1.5, n = 53).

Related to pedal length proportions, it is also possible to assess the relative mechanical advantage of the triceps surae muscle at heel off, modeling the TMT as a second class lever with the fulcrum at the MT-1 head, and the load at the mid talar trochlea (Martin, 2011; see Fig. S16,

Table S13). The Feet A ratio is 0.690, compared to 0.710 (± 0.028, n = 7) for E/MUP humans and 0.713 (± 0.019, n = 65) for a recent human sample. A pooled Middle Paleolithic sample provides similar ratios (0.692 ± 0.026, n = 8).

3.2.2 Talocrural Morphology

The tibial articulations of the Cro-Magnon 4337 and 4338 tali exhibit the anterior extensions of the trochleae and the medial malleolar facets, which are present on most Late Pleistocene tali (Table S1; Figs. 3 and 5) and reflect frequent talocrural dorsiflexion. The CM 4338 talus has only a suggestion of a lateral squatting facet, but a clear one is present on the laterodorsal neck of the CM 4337 talus. The facet on CM 4337 matches closely with the anterior articular rounding of CM 4330 distal tibia (with which it articulates), and a similar squatting facet is present on the antimere of CM 4330, CM 4333 (Fig. S2). Similar evidence of squatting as an habitual resting position is present for approximately half of the E/MUP talocrural articulations, lower than the overall Middle Paleolithic frequency of 77.8% (Table 2).

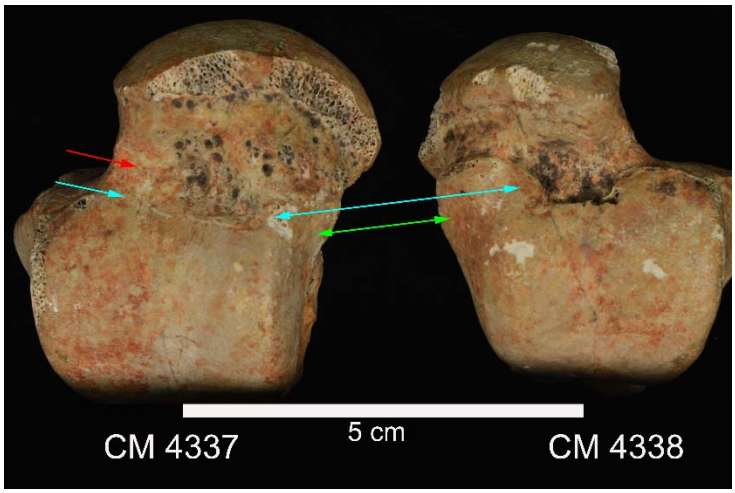

Figure 5. Dorsodistal views of the Cro-Magnon tali, showing the medial malleolar (green arrow) and medial trochlear (blue arrow) extensions on both tali and the lateral trochlear extension (blue arrow) and squatting facet (red arrow) on CM 4337.

Table 2. Pedal discrete trait presence/absence for the Cro-Magnon remains and comparative Late Pleistocene samples, provided as the frequency of presence (n).[1]

	Lateral Squatting Facet[2]	Sulcus Tali Facet	Talo-calcaneal Facet Fusion[2,3]	Naviculo-cuboid Facet	Metatarsal 1-2 Facet
CM 4337	present	present	present		
CM 4338	absent	present	present		
CM 4336			present		
CM 4339				absent	
CM 4340				present	
CM 4341				present	
CM 4345bis					absent
CM 4346					absent
E/MUP	55.0% (20)	35.7% (14)	88.9% (18)	50.0% (12)	12.5% (8)
MPMH	100% (6)	40.0% (5)	100% (4)	100% (3)	66.7% (3)
Neandertals	71.4% (21)	41.2% (17)	86.8% (19)	71.4% (7)	41.7% (12)

[1] E/MUP: Early/Mid Upper Paleolithic humans; MPMH: Middle Paleolithic modern humans; insufficient Late Upper Paleolithic data are available (cf. Trinkaus, 2015). For frequency data on diverse recent human samples, see Trinkaus et al. (2014).

[2] The presence / absence of squatting facets pools together observations from tali and distal tibiae, and the presence of talocalcaneal facet fusion includes observations from tali and calcanei.

[3] Talocalcaneal facet fusion refers only to fusion of the anterior and medial facets; additional fusion to the posterior facet occurs but is not considered here.

The size of the talar trochlea relative to talar length, which is also reflected (inversely) in the relative length of the talar head and neck (Rhoads and Trinkaus, 1977), provides an indication of articular hypertrophy. The distribution of trochlear length versus talar length (Fig. 6) provides only partial separation of the Late Pleistocene samples, despite the relatively longer trochleae (and hence "short" talar necks) among the Neandertals relative to the E/MUP sample. The one E/MUP talus with a relatively long trochlea is Mladeč 30, and it is joined by four of the LUP tali. CM 4337 falls with the larger E/MUP tali, and CM 4338 is among the smaller ones with relatively shorter trochleae. Neither one of the Cro-Magnon tali has a particularly long, or large, trochlea, and hence (contra Vallois and Billy, 1965) neither one has a relatively short talar neck (see also Table S1).

However, if the average of the trochlear length and breadth (and hence a more complete measure of trochlear size) is compared to talar length (Fig. 6), the sample differences largely

disappear. CM 4337 remains in the middle of the E/MUP sample, and CM 4338 has one of the relatively smallest trochleae.

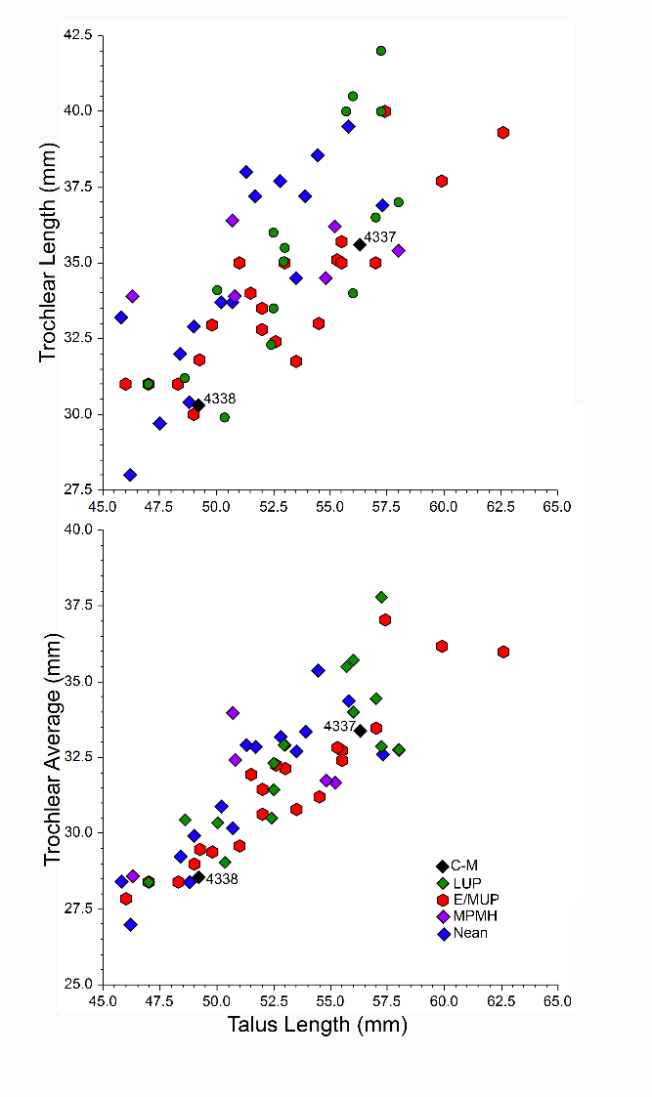

Figure 6. Bivariate plots of trochlear length (above) and the geometric mean of trochlear length and breadth (below) versus talar length for the Cro-Magnon tali and comparative Late Pleistocene tali. Sample abbreviations as in Fig. 4.

3.2.3 Pedal Arches

The articulation of the Feet A bones (especially of the cuboid and cuneiform bones) provides it with a normal transverse pedal arch. The presence of such an arch is evident in Feet B from the horizontal and vertical orientations of the MT-4 tarsal facets, such that they face medially and plantarly respectively (Morton, 1922-24; Ward et al., 2011; Table S7). Both of these orientations reflect the dorsal convexity of the lateral TMT articulations and elevation of those joints from the plantar plane. The Feet B MT-4 horizontal angles (68°, 71°) are modestly below the values for the available E/MUP MT-4s (77.9° ± 3.9°, n = 5) and those of a recent

human sample (79.5° ± 4.5°, n = 40). Their vertical angles (75°, 79°) are similar to the two other available E/MUP values (76°, 84°) and those of a recent human sample (77.8° ± 4.8°, n = 40).

A more indirect indication of the presence of pedal arches is the talar head torsion angle, in which angles substantially greater than zero serve to stabilize the transverse tarsal articulation in supination (Elftman, 1960; Martin, 2011). The values for the two Cro-Magnon tali (31°, 36°) are in the middle of an E/MUP sample (35.4° ± 4.7°, n = 10) and well within the range of a pooled recent human sample (41.9° ± 7.3°, n = 140). Therefore, despite the relatively low pedal arch produced by the virtual assembly of the Feet A bones (Fig. S16), these skeletal features indicate normal human pedal arches for the Cro-Magnon feet.

3.2.4 Subtalar Morphology

The Cro-Magnon tali and calcaneus have fully fused anterior and medial talocalcaneal facets [as noted by Vallois and Billy (1965)] (Figs. 3, S1 and S4), as do ≈90% of Late Pleistocene tali and calcanei (Table 2). The sides of the fused facets on the tali have a protuberance into the sulcus tali, especially on CM 4337, and the CM 4336 facet has a small notch along the posterolateral side. In both cases, the anterolateral to posteromedial articular profile is a smooth curve, indicating little restriction on talocalcaneal rotation (or pronation / supination).

These surfaces are joined by large and prominent sulcus tali facets on each of the Cro-Magnon tali (Fig. S3), facets which traversed most of the anterolateral margins of the posterior calcaneal facets. Similar, but generally smaller, sulcus tali facets are present in 30%-40% of Late Pleistocene tali (Table 2), frequencies similar to recent human samples (Trinkaus, 1975b). As with the Cro-Magnon anterior malleolar and trochlear extensions and the CM 4337 squatting facet, they indicate habitual talocrural and subtalar dorsiflexion (Morimoto, 1960).

Late Pleistocene humans have a modest medial positioning of the acetabulum pedis, as is reflected in the talar head-neck angle and the medial projection of the sustentaculum tali. The Cro-Magnon tali have relatively low talar neck angles (Table S1; Fig. 7), but ones well with Late Pleistocene and recent human ranges of variation. An index of sustentacular projection versus calcaneal body breadth is 52.5 for CM 4336, which is in the middle of the Late Pleistocene variation (Fig. 7).

More distally, the CM 4340 navicular bone and the CM 4341 cuboid bone exhibit naviculocuboid facets, whereas the CM 4339 navicular bone lacks one. The one on the cuboid bone in particular is relatively large (Figs. 3 and S6), as opposed to the small ones present on most other Late Pleistocene and recent humans; one exception is the very large ones of Pavlov 37 (Trinkaus et al., 2017). Such facets, as opposed to a ligamentous surface, are moderately common among Late Pleistocene humans (Table 2). The Cro-Magnon subtalar articulations are therefore similar to those of other Late Pleistocene (and recent) humans, being notable primarily for the large sizes of their sulcus tali facets and of the CM 4341 naviculocuboid facet.

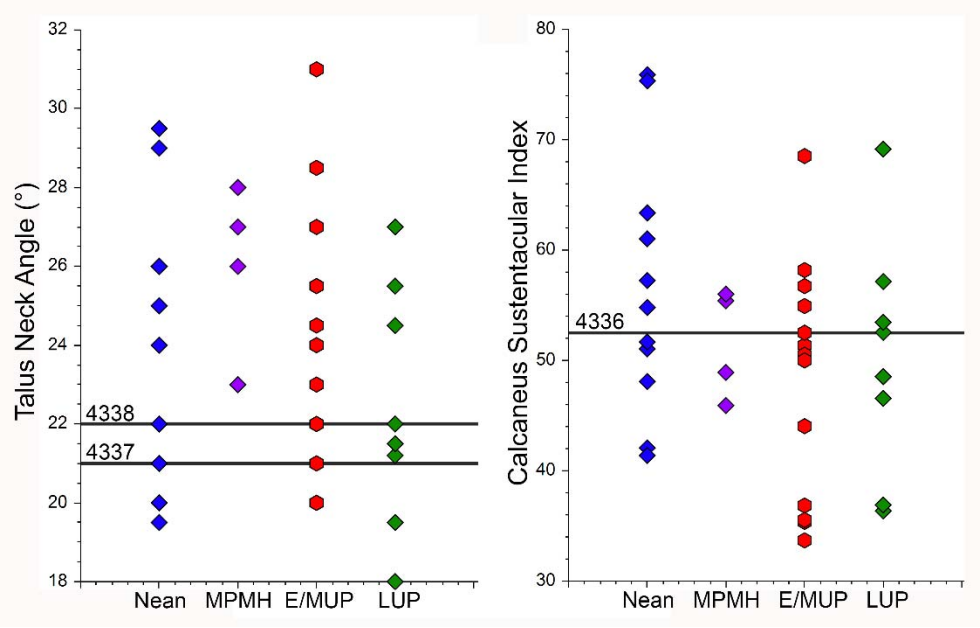

Figure 7. Medial displacement of the acetabulum pedis. Talus neck angle (left) and calcaneus sustentacular index (sustentacular breadth versus body breadth) (right). Sample abbreviations as in Fig. 4.

3.2.5 Hallucal Considerations

The distal (metatarsal) facet of the CM 4342 medial cuneiform is flat dorsally, but it is modestly convex plantarly, with a slight twist to the facet. The plantar half of the surface points directly distally, but the flatter dorsal half is oriented slightly medially (Fig. S7). Corresponding to this, the preserved medial portion of the CM 4345 MT-1 proximal articulation presents minimal concavity (Fig. S8). The articulation therefore indicates little interlocking of the

tarsometatarsal articulation. In contrast, the proximal articulation of the CM 4345bis MT-1 is distinctly concave transversely. Its lateral side has a proximal projection slightly plantar of its dorsoplantar middle, one which would have formed a close-packed position with the medial cuneiform during heel-off (Fig. S8).

The lateral base of the CM 4345 MT-1 is insufficiently preserved to indicate whether an MT-1/MT-2 facet was present. However, both the CM 4345bis MT-1 and CM 4346 MT-2 indicate that such a facet was absent from at least the right foot of Feet B. However, such facets are present in only 36.4% (n = 22) of Late Pleistocene individuals preserving one or both sides of the region (Table 2), a frequency which is nonetheless above those of recent human samples (Trinkaus et al., 2014). The Cro-Magnon hallucal tarsometatarsal remains therefore indicate fully adducted halluces, as is evident in the virtual assembly of the Feet A remains (Fig. 1).

Distally, the plantar intersesamoid crest of CM 4345bis provides a horizontal head angle (between the crest axis and the diaphyseal axis) of 8° (the one for CM 4345 is abraded) (Fig. 8). The angle indicates a normal level of lateral deviation at the metatarsophalangeal articulation for Feet B (Meyer, 1979). The value is similar to those of the few other E/MUP humans providing the angle (4.7° ± 3.1°, 0° - 9°, n = 6), similar to a pooled Middle Paleolithic sample (6.3° ± 3.4°, n = 11), and modestly above a recent human sample (3.4° ± 2.5°, n = 40).

Figure 8. The CM 4345bis MT-1 in plantar view (left) and the CM 4351 PP-1 in dorsal view (right). Note the lateral deviation of the MT-1 intersesamoid crest (arrow) and the left deviation of the phalanx relative to the transverse plane of its proximal articulation.

Lateral deviation at the hallucal metatarsophalangeal articulation may also be indicated by the base of the proximal phalanx (PP-1; CM 4351). The proximal articulation deviates distinctly to the left in dorsal view (Fig. 8). If the bone is indeed a left, then it would provide

evidence for normal hallucal orientation. At the same time, the (albeit pathological) distal articulation deviates to the right in dorsal view relative to the shaft, which would reinforce lateral hallucal deviation if the bone were a right.

3.2.6. Body Size Indications

The pedal remains from Cro-Magnon, and especially those of Feet A and B, can provide indications of the individuals' statures, based on regressions derived from recent human samples (Byers et al., 1989; Cordeiro et al., 2009; Pablos et al., 2013; Table S14). Using talar, calcaneal and/or metatarsal lengths, the available formulae provide average estimates of 173.9 cm (172.6–175.6 cm) for Feet A, 170.8 cm (166.7–174.4 cm) for Feet B, and 166.9 cm for Feet C. These values are in agreement, given standard errors of 3–6 cm in the estimates, with the estimated stature ranges based on femoral and tibial lengths (Thibeault and Villotte, 2018) of 170–177 for Alpha (or Feet B), 161–167 cm for Beta (or Feet C), and 167–174 cm for Gamma (or Feet A).

Although it is possible to estimate body mass from overall foot dimensions (Ruff et al., 2021), the incomplete nature of the Cro-Magnon associated foot skeletons prevents reliable estimation of foot length and especially breadth. More reliable estimates are possible for these Cro-Magnon individuals from their femoral head diameters (Table S10; Ruff et al., 2018).

3.3. Paleopathology

On the 17 bones under study, and apart from minor degenerative changes (see SI) likely related to the advanced age of most of the adult sample (Gambier et al., 2006; Thibeault and Villotte, 2018; Trinkaus et al., 2021), few pathological changes were recorded. The main ones concern the CM 4347 MT-4, the CM 4349 MT-5, and the CM 4351 PP-1 (Fig. 9; see also Figs. S10 to S12), all associated in Feet B (Alpha/Cro-Magnon 1). An alteration of the gross morphology of the distal extremity is present on all three bones. These alterations are, in the three cases, very similar:

- no major erosive or proliferative lesions are visible;
- the original gross morphology of the head is altered, leading to a flattened head;
- the regularity of the convex surface is altered, leading to a "bumpy" articular surface;
- well circumscribed openings (with smooth margins) are present on the articular surface;
- for the two metatarsals, each of these openings leads to a cul-de-sac;

- for the proximal hallucal phalanx the opening reaches a subchondral cyst (Fig. S12);

- in each case, the margins of the lesion are very well defined and clearly sclerotic.

Considering the absence of eburnation and proliferative lesions, osteoarthritis appears as an improbable diagnosis. In the same vein, the lack of major erosive lesions makes unlikely a diagnosis of erosive arthropathies, such as spondylarthropathies or gout. In his review of the pathological lesions in Cro-Magnon assemblage, Dastugue (1967) mentioned only the alteration of the distal extremity of the proximal phalanx, and referred it to trauma or an infection. An alternative would be to link these alterations to the systemic condition affecting Alpha/Cro-Magnon 1 (see Dastugue, 1967; Thillaud, 1985), considering the homogeneity of the changes and their aspect that indicates a long-standing condition.

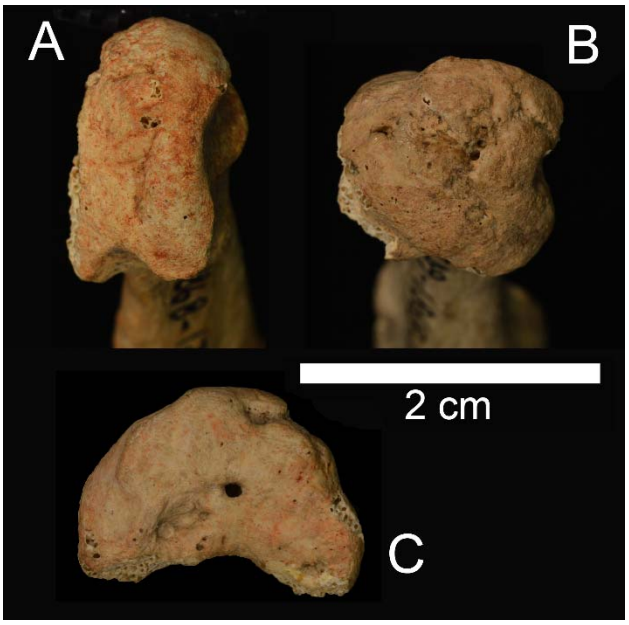

Figure 9. Pathological alterations of the distal articulations of the CM 4347 metatarsal 4 (A), the CM 4349 metatarsal 5 (B), and the CM 4351 proximal hallucal phalanx (C).

Pathological alterations affect two other bones. The CM 4341 left cuboid bone displays extra bone production similar to that from a periosteal reaction on its dorsal surface, and it has many deep and small resorptive areas with rounded (i.e. remodeled) exposed trabeculae within the depressions (Fig. S6). Finally, the CM 4347 MT-4 exhibits, on the medial surface of the proximal shaft, two round well-circumscribed depressions (Fig. S10). These changes of unknown origin resemble alterations on both fifth metatarsals of the MUP Baousso da Torre 1 (Villotte et al., 2017).

4. Discussion and Conclusion

In the context of disentangling the mixed human remains from the Abri de Cro-Magnon, the surviving tarsals, metatarsals and phalanx can be associated into the three postcranial individuals identified from the lower limb bones by Thibeault and Villotte (2018). As a result, rather than being treated solely as isolated elements in comparative analyses of Late Pleistocene pedal remains (e.g., Trinkaus et al., 2014; Pablos et al., 2017), it is now possible to assess within-foot proportions for additional earlier Upper Paleolithic individuals. Moreover, the proximal calcaneus to distal MT-1 Feet A (or Gamma) pedal skeleton adds to the small sample of such Late Pleistocene pedal skeletons, permitting further documentation of recent human foot and foot-to-leg proportions through the Late Pleistocene.

The talocrural and subtalar articulations present little of note for an earlier Upper Paleolithic, or Late Pleistocene, human. The anterior trochlear extensions of the tali are common among these samples (Trinkaus, 1975b; Trinkaus et al., 2014), and the presence of a squatting facet on one but not the other of the Cro-Magnon tali matches their presence in approximately half of the E/MUP individuals. Sulcus tali facets are moderately common in the E/MUP and Middle Paleolithic samples, but the Cro-Magnon ones are notable for their large sizes. All of these features reflect habitual talocrural and subtalar dorsiflexion, through locomotion and squatting.

The Feet B (or Alpha/Cro-Magnon 1) distal MT-4, MT-5 and PP-1 pathological alterations are of unclear etiology, but they probably reflect one of the manifestations of the systemic abnormalities of Cro-Magnon 1. The other pedal pathological changes are minor, and none of them appear to have affected the basic functioning of these feet.

The reassessment of the Cro-Magnon pedal remains therefore adds to the sorting by individual of the Cro-Magnon human assemblage, after 150+ years of unclear associations. Morphologically these foot bones reinforce pedal patterns emerging among earlier Upper Paleolithic, and later Pleistocene generally, human remains.

5. Acknowledgments

The authors thank Veronique Laborde, Aurélie Fort (curators at the Musée de l'Homme) and Dominique Grimaud-Hervé (in charge of the collection) for granting access to the Cro-Magnon remains. A. Pablos kindly provided comparative recent human pedal data. Many

colleagues and curators have provided access to Late Pleistocene comparative pedal remains. To all we are grateful. Funding: This research was supported by ANR Gravett'Os (ANR-15-CE33-0004). The funding agency had no role in the research design or publication.

6. References

Auerbach, B.M., Ruff, C.B., 2006. Limb bone bilateral asymmetry: variability and commonality among modern humans. J. Hum. Evol. 50: 203-218. https://doi.org/10.1016/j.jhevol.2005.09.004.

Barnett, C.H., 1954. Squatting facets on the European talus. J. Anat. 88, 509–513. PMCID: PMC1244661.

Bräuer, G., 1988. Osteometrie. in: Knussman, R. (Ed.) Anthropologie I. Fischer, Stuttgart. pp. 160-232.

Broca, P., 1868. Sur les crânes et ossements des Eyzies. Bull. Soc. Anthropol. Paris 3, 350–392. https://doi.org/10.3406/bmsap.1868.9548

Byers, S., Akoshima, K., Curran, B., 1989. Determination of adult stature from metatarsal length. Am. J. Phys. Anthropol. 79, 275-279. https://doi.org/10.1002/ajpa.1330790303

Cordeiro, C., Muñoz-Barús, J.I., Wasterlain, S., Cunha, E., Vieira, D.N., 2009. Predicting adult stature from metatarsal length in a Portuguese population. Forensic Sci. Intl. 193, 131.e1-131.e4. https://doi.org/10.1016/j.forsciint.2009.09.017.

Dastugue J., 1967. Pathologie des hommes fossiles de l'Abri de Cro-Magnon. L'Anthropol. 71, 479-492.

Elftman, H., 1960. The transverse tarsal joint and its control. Clin. Orthop. 16, 41-46.

Gambier, D., Brůžek, J., Schmitt, A., Houët, F., Murail, P., 2006. Révision du sexe et de l'âge au décès des fossiles de Cro-Magnon (Dordogne, France) à partir de l'os coxal. C. R. Palevol 5, 735-741. https://doi.10.1016/j.crpv.2005.12.011.

Holt, B., Formicola, V., 2008. Hunters of the Ice Age: The biology of Upper Paleolithic people. Yrbk. Phys. Anthropol. 51, 70-99. http://doi.10.1002/ajpa.20950.

Lartet, L., 1868. Une sépulture des troglodytes du Périgord (crânes des Eyzies). Bull. Soc. Anthropol. Paris 3, 335–349. https://doi.org/10.3406/bmsap.1868.9547

Martin, R.L., 2011. The ankle and foot complex. in: Levangie, P.K., Norkin, C.C. (Eds.) Joint Structure and Function 5th ed. F.A. Davis, Philadelphia, pp. 440-481.

Meyer, M., 1979. A comparison of hallux abducto valgus in two ancient populations. J. Am. Pod. Assoc. 69, 65-68. http://doi.10.7547/87507315-69-1-65.

Morimoto, I., 1960. The influence of squatting posture on the calcaneus in the Japanese. Formation of the forward extension complex of the posterior talar articular surface. J. Anthropol. Soc. Nippon 68, 16-22. https://doi.org/10.1537/ase1911.68.16.

Morton, D.J., 1922-24. Evolution of the human foot. Am. J. Phys. Anthropol. 5, 305-336; 7, 1-52.

NCSS, 2016. NCSS 11 Statistical Software. Kaysville, Utah: NCSS, LLC.; ncss.com/software/ncss.

Pablos, A., Gómez-Olivencia, A., Garcia-Pérez, A., Martínez, I., Lorenzo, C., Arsuage, J.L., 2013. From toe to head: Use of robust regression methods in stature estimation based on foot remains. Forensic Sci. Intl. 296, 229.e1-299.e7. https://doi.org/10.1016/j.forsciint.2013.01.009.

Pablos, A., Pantoja-Pérez, A., Martínez, I., Lorenzo, C., Arsuaga, J.L., 2017. Metric and morphological analysis of the foot in the Middle Pleistocene sample of Sima de los Huesos (Sierra de Atapuerca, Burgos, Spain). Quatern. Intl. 433, 103-113. http://dx.doi.org/10.1016/j.quaint.2015.08.044.

Partiot, C., Trinkaus, E., Knüsel, C.J., Villotte, S., 2020. The Cro-Magnon babies: Morphology and mortuary implications of the Cro-Magnon immature remains. J. Archaeol. Sci. Rep. 30, 102257. https://doi.org/10.1016/j.jasrep.2020.102257.

Pruner-Bey, F., 1865-75. An account of the human bones found in the cave of Cro-Magnon, in Dordogne, in: Lartet, E., Christy, H. (Eds.), Reliquiae Aquitanicae: Being Contributions to Archaeology and Palaeontology of Périgord and the Adjoining Provinces of Southern France. Williams and Norgate, London, pp. 73–92.

Rhoads, J.G., Trinkaus, E., 1977. Morphometrics of the Neandertal talus. Am. J. Phys. Anthropol. 46, 29-44. http://doi/10.1002/ajpa.1330460106 .

Ruff, C.B., Burgess, M.L., Squyres, N., Junno, J.A., Trinkaus, E., 2018. Lower limb articular scaling and body mass estimation in Pliocene and Pleistocene humans. J. Hum. Evol. 115: 85-111. https://doi.10.1016/j.jhevol.2017.10.014.

Ruff, C.B., Wunderlich, R.E., Hatala, K.G., Tuttle, R.H., Hilton, C.E., D'Août, D.M., Webb, D.M., Hallgrímsson, B., Mushiba, C., Kaksh, M., 2021. Body mass estimation from

footprint size in hominins. J. Hum. Evol. 156, 102997. https://doi.org/10.1016/j.jhevol.2021.102997.

Thibeault, A., Villotte, S., 2018. Disentangling Cro-Magnon: A multiproxy approach to reassociate lower limb skeletal remains and to determine the biological profiles of the adult individuals. J. Archaeol. Sci. Rep. 21, 76-86. https://doi.org/10.1016/j.jasrep.2018.06.038.

Thillaud, P.L., 1985. L'homme de Cro-Magnon et ses maladies. Les dossiers d'archéologie 97, 67–73.

Trinkaus, E., 1975a. A Functional Analysis of the Neandertal Foot. PhD. Thesis, University of Pennsylvania.

Trinkaus, E., 1975b. Squatting among the Neandertals: A problem in the behavioral interpretation of skeletal morphology. J. Archaeol. Sci. 2, 327-351. https://doi.org/10.1016/0305-4403(75)90005-9.

Trinkaus, E., 1978. Bilateral asymmetry of human skeletal non-metric traits. Am. J. Phys. Anthropol. 49, 315-318. http://doi/10.1002/ajpa.1330490304.

Trinkaus, E., 2006. Body length and body mass. in: Trinkaus, E., Svoboda, J.A. (Eds.) Early Modern Human Evolution in Central Europe: The People of Dolní Věstonice and Pavlov. Oxford University Press, New York. pp. 233-241.

Trinkaus, E., 2015. The appendicular skeletal remains of Oberkassel 1 and 2. in: Giemsch, L., Schmitz, R.W. (Eds.) The Late Glacial Burial from Oberkassel Revisited. Verlag Phillip von Zabern, Darmstadt. pp. 75-132.

Trinkaus, E., Buzhilova, A.P., Mednikova, M.B., Dobrovolskaya, M.V., 2014. The People of Sunghir: Burials, Bodies and Behavior in the Earlier Upper Paleolithic. Oxford University Press, New York.

Trinkaus, E., Wojtal, P., Wilczyński, J., Sázelová, S., Svoboda, J., 2017. Palmar, patellar and pedal human remains from Pavlov. PaleoAnthropology 2017, 73-101. . http://doi.10.4207/pa.2017.art106 .

Trinkaus, E., Lacy, S.A., Thibeault, A., Villotte, S., (2021) Disentangling Cro-Magnon: The dental and alveolar remains. J. Archaeol. Sci. Rep. 37, 102991. http://doi.org/10.1016/j.jasrep.2021.102911.

Vallois, H.V., Billy, G., 1965. Nouvelles recherches sur les hommes fossiles de l'abri de Cro-Magnon. L'Anthropol. 69, 47–74.

Villotte, S., Balzeau, A., 2018. Que reste-t-il des hommes de Cro-Magnon 150 ans après leur découverte? Bull. Soc. Anthropol. Paris 30, 146–152. https://doi.org/10.3166/bmsap-2018-0026.

Villotte, S., Thibeault, A., Sparacello, V., Trinkaus, E., 2020. Disentangling Cro-Magnon: The adult upper limb skeleton. J. Archaeol. Sci. Rep.33, 102475. https://doi.org/10.1016/j.jasrep.2020.102475.

Ward, C.V., Kimbel, W.H., Johanson, D.C., 2011. Complete metatarsal and arches in the foot of *Australopithecus afarensis*. Science 331, 750-753. http://doi.10.1126/science.1201463.

Disentangling Cro-Magnon: The Pedal Remains
Supporting Information

Erik Trinkaus, Adrien Thibeault, and Sébastien Villotte

S1: The Cro-Magnon Pedal Remains

The Cro-Magnon lower limb sample includes nine tarsals, seven metatarsals and one proximal pedal phalanx. All of these bones are largely complete, but they have variably sustained minor damage. They are presented in terms of preservation, salient morphology, and any pathological lesions. For each bone standard osteometrics are tabulated, largely following the Martin system (Bräuer, 1988) but including other measurements that have been employed in descriptions of Late Pleistocene pedal remains [see, for example, Matiegka (1938), Trinkaus (1975a), Trinkaus et al. (2014, 2017) and Villotte et al. (2017)]. Non-metric traits follow these authors and/or are referenced in the tables. Measurements with minor estimation are in parentheses.

It is possible to associate these pedal remains reliably into three "feet", designated Feet A, B and C (see text 3.1 and below). The attribution by Feet A, B or C is provided for each bone with its description, with tentative attributions indicated, and the rationales for the associations are provided in the text. As previously noted in the disentangling of the Cro-Magnon lower limb remains (Thibeault and Villotte, 2018), the CM 4337 talus and the CM 4336 calcaneus (Feet A) can be associated with individual Gamma on the basis of articular congruence. It is likely, based on size and pathology, that Feet B is associated with individual Alpha and that Feet C is associated with individual Beta (see text 3.1.5 and Table S12), but these cannot be confirmed by articular congruence.

S2: The Cro-Magnon Tali

S2.1. Cro-Magnon 4337 Left Talus (Feet A)

S2.1.1 Preservation:

The bone is complete with minor damage (Fig. S1). The medial tubercle is broken. The margin of the head is eroded dorsally and plantarly. There are areas of abrasion of the anterior and medial facets for the calcaneus. The margin of the posterior facet for the calcaneus is eroded laterally and medially.

S2.1.2 Morphology:

On the dorsal neck (Figs 5 and S1) there is a modest distal extension of the medial malleolar facet. There is a suggestions of a medial trochlear distal extension alongside of the malleolar facet, but it is insufficient to be scored as present (see Table S1). Laterally there is a distal trochlear extension, which leads into a distinct lateral squatting facet (contra Vallois and Billy, 1965). The facet articulates with the distinct rounding of the lateral portion of the anterior distal articular border of the CM 4330 tibia (Fig. S2).

The anterior and medial calcaneal facets are completely fused with an even concave longitudinal curve (Fig. S1). In the middle of the fused facets there is a large articular projection into the sulcus tali, projecting up to ≈5.4 mm and 11 mm long. The articular extension is set on a pillar of bone going to the plantar side of the head.

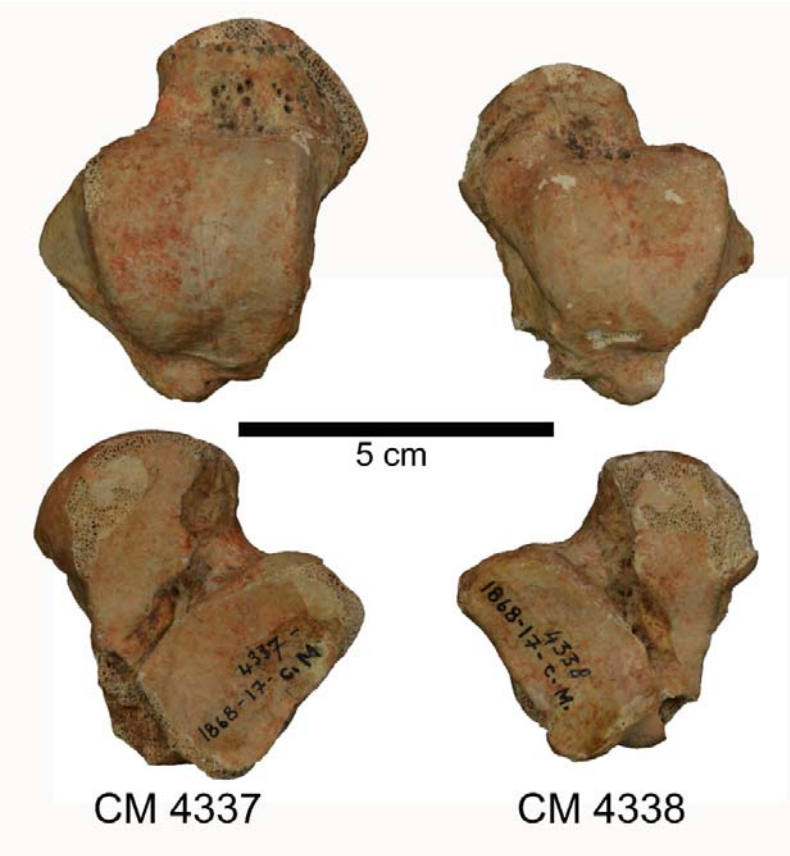

Figure S1. Dorsal (above) and plantar (below) views of the Cro-Magnon 4337 (left) and 4338 (right) tali.

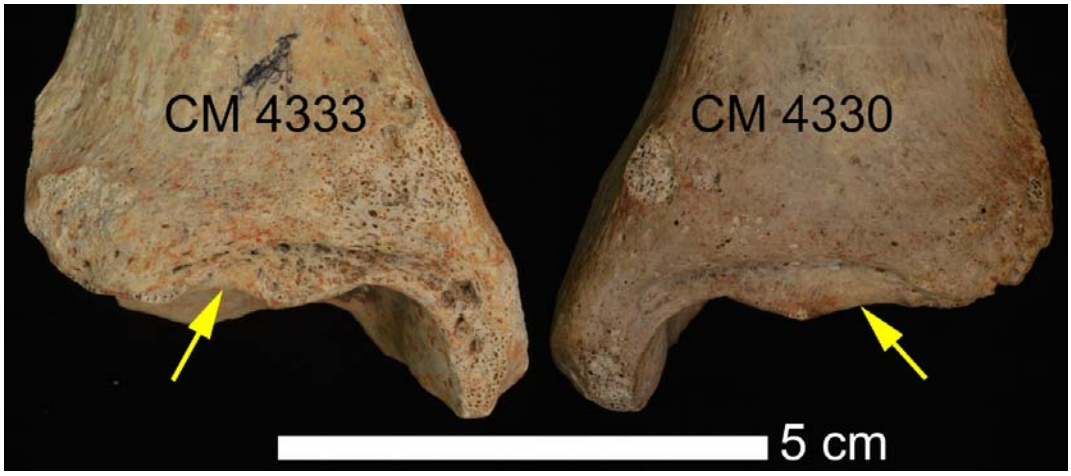

Figure S2. Anterior views of the Cro-Magnon 4330 and 4333 tibia, both attributed to individual Gamma (Thibeault and Villotte, 2018). Each one exhibits a small lateral articular margin rounding (yellow arrows) that can be seen as a tibial squatting facet. The one on CM 4330 extends 3.2 mm from the trochlear surface and is 11.5 mm wide. The similar one on CM 4333 extends 4.1 mm from the trochlear surface and is 10.7 mm wide. The one on CM 4330 articulates with the lateral squatting facet on CM 4337.

The sulcus tali presents a distinct sulcus tali facet (Fig. S3). It extends up to 7.5 mm from the posterior calcaneal surface margin. The rounded swelling for it increases from the middle of the posterior calcaneal border to the lateral posterior calcaneal border, but the hemi-ovoid facet is basically below the lateral malleolar area. It is therefore triangular with a rounded lateral end, although its medial end is eroded.

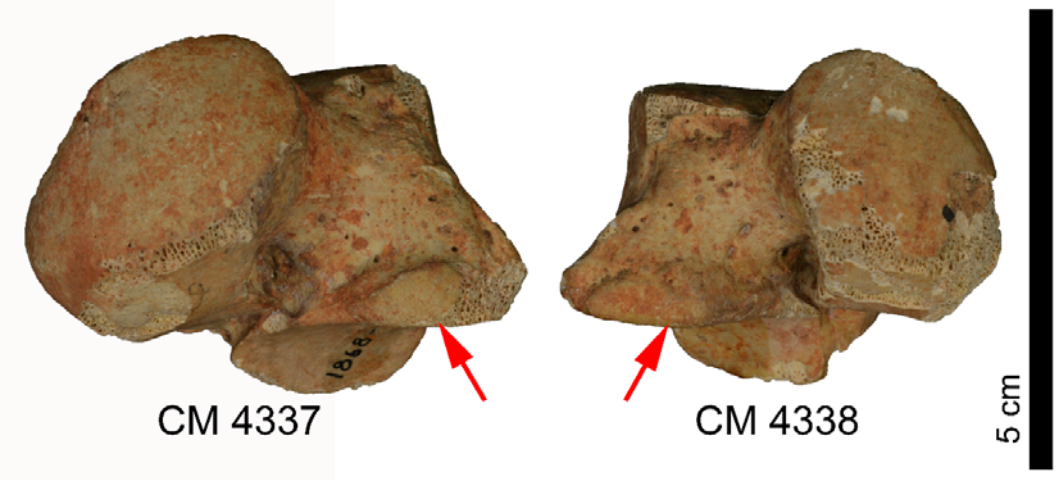

Figure S3. Distolateral views of the Cro-Magnon 4337 and 4338 tali, with their prominent sulcus tali facets [*facies externa accessoria corporis tali* of Sewell (1904-05); see also Morimoto (1960) and Trinkaus (1975b)] evident on each one (arrows).

S2.1.3. Paleopathology

Except for slight lipping on the dorsal edge of the sulcus tali facet, there are no signs of articular or periarticular changes on CM 4337.

S2.2 Cro-Magnon 4338 Right Talus (Feet C)

S2.2.1 Preservation

The bone is largely complete with marginal erosion (Fig. S1; Table S1). The medial tubercle is broken. The articular surface of the head is eroded, especially plantarly extending onto the anterior calcaneal facet.

S2.2.2 Morphology

The anterior and medial calcaneal facets are fully fused and exhibit an even curve (Fig. S1), which is evident despite the erosion below the head. There is an articular protrusion into the sulcus tali in the middle of the combined facet. It is smaller than the one on CM 4337, and it does not rest on a swelling of bone above into the sulcus tali. It projects 2.8 mm into the sulcus tali from the articular contour.

The dorsal neck of CM 4338 exhibits distal extensions of the medial malleolar surface, and of both the medial and lateral sides of the trochlea (Fig. S1). These articular extensions indicate habitual talocrural dorsiflexion. However, the area for a lateral squatting facet has only a slight smoothing of the surface without the presence of a clear squatting facet. It may represent an incipient squatting facet, but it is not as well developed as the one on CM 4337. The squatting facet is therefore scored as absent (Table S1).

As with CM 4337, the posterior side of the sulcus tali exhibits a prominent sulcus tali facet (Fig. S3). It extends up to 5.6 mm from posterior calcaneal surface margin, and it is 13.8 mm wide. The whole swelling begins at the medial end of the sulcus tali, but the distinct portion of the facet is lateral, below the lateral malleolar area.

S2.2.3. Paleopathology

With the exception of slightly lipping on the lateral trochlear extension margin, there is no evidence of articular or periarticular alterations on CM 4338.

Table S1. Osteometrics of the Cro-Magnon tali, in millimeters and degrees. M#: Martin measurement numbers following Bräuer (1988). Letters for discrete traits follow Barnett (1954).

	M#	***CM 4337***	***CM 4338***
Length	1	56.3	49.2
Medial maximum length		56.0	--
Lateral maximum length	1a	60.8	54.9
Maximum height	3	32.9	29.6
Articular height	3b	29.0	26.2
Articular breadth	2b	49.8	45.5
Trochear length	4	35.6	30.3
Trochlear breadth	5	31.3	26.9
Anterior trochlear breadth	5(2)	32.2	27.5
Posterior trochlear breadth	5(1)	27.6	23.8
Trochlear height	6	10.6	7.8
Lateral malleolar height		25.5	22.5
Lateral malleolar oblique height	7	28.2	23.7
Head-neck length	8	22.5	18.5
Head length	9	36.2	33.5
Head breadth	10	23.9	22.4
Posterior calcaneal length	12	(35.0)	32.7
Posterior calcaneal breadth	13	24.6	20.7
Trochlear angle		18°	13°
Neck Angle	16	21°	22°
Torsion angle	17	31°	36°
Posterior calcaneal angle	15	49°	44°
Medial malleolar extension	B	pres	pres
Medial trochlear extension	C	abs	pres
Lateral trochlear extension	D	pres	pres
Lateral squatting facet	F	pres	abs
Sulcus tali facet (see Fig. S3)		pres	pres
Anterior-medial calcaneal facet fusion		pres	pres

S3: The Cro-Magnon Calcaneus

S3.1 Cro-Magnon 4336 Right Calcaneus (Feet A)

S3.1.1 Preservation

The bone (Fig. S4; Table S2) presents largely complete articular facets, tuberosity, sustentaculum tali, and medial surface bone. However, about three-quarters the cortical bone of the lateral surface is absent, with more substantial destruction (both cortical and subchondral) on the middle of the surface. The margin of the tuberosity is heavily abraded, especially dorsally, and there is minor erosion of the posterior and lateral margins of posterior talar facet. There is also abrasion of the posterior tip of the medial talar facet and the adjacent sustentaculum tali.

S3.1.2 Morphology

There is clear separation of the medial and posterior talar facets, but the anterior and medial ones are fused, providing an even articular curve. There is evidence of the fusion of these two surfaces in a slight notch anteromedially and a much larger one posterolaterally, with a slightly raised area on the posterolateral margin.

The medial process large and broad, but it only projects modestly more than the plantolateral tuberosity. The flexor hallucis longus sulcus on the plantar sustentaculum tali is single, 9.2 mm wide, and relatively smooth with cross-striations.

S.3.1.3 Paleopathology

There are no evident degenerative changes. The triceps surae tendon insertion on the tuberosity is evident but small, not a real enthesophyte, with clear demarcations of the tendon and bursae attachments. There are no changes at the plantar fascia enthesis.

Figure S4. Dorsal (left) and medial (right) views of the Cro-Magnon right calcaneus.

Table S2. Osteometrics of the Cro-Magnon 4336 calcaneus, in millimeters and degrees.

	M#			*M#*	
Maximum length	1	80.4	Medial process length[1]		30.0
Total length	1a	76.9	Posterior talar length	9	35.8
Body length	5	60.0	Posterior talar breadth	10	24.6
Median breadth	2	42.1	Deflex angle	14	40°
Sustentacular breadth	6	14.5	Anterior talar breadth[2]		13.4
Tuberosity height	7	(45.5)	Medial talar breadth[2]		14.2
Tuberosity breadth	8	32.0	Ant-med. notch breadth[2]		9.1

[1] Distal projection, from the proximal tuberosity, of the plantar medial process.

[2] Maximum breadths of the anterior and medial talar facet and minimum breadth of the articular notch at their union.

S4: The Cro-Magnon Anterior Tarsal Bones

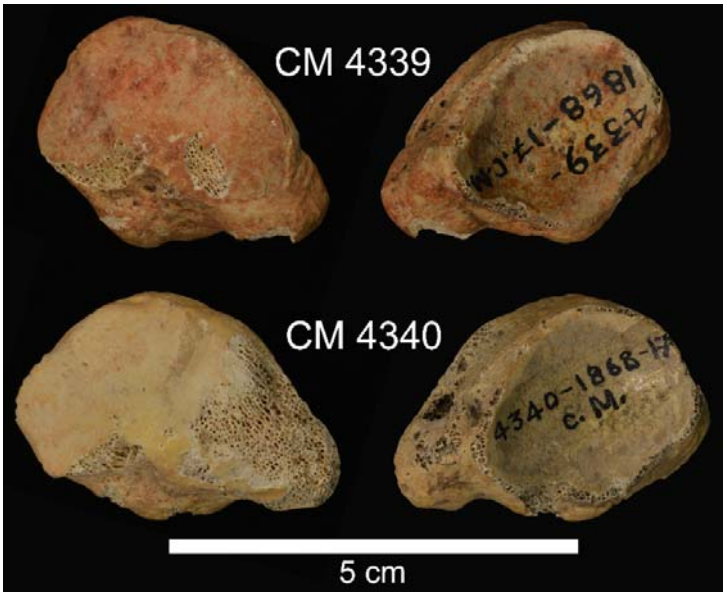

Figure S5. Distal (left) and proximal (right) views of the Cro-Magnon 4339 and 4340 right navicular bones.

S4.1 Cro-Magnon 4339 Right Navicular Bone (Feet C)

S4.1.1 Preservation

The bone is complete with minor damage (Fig. S5; Table S3). The plantar tip of the tuberosity is missing. There is erosion of the plantar margin of the lateral cuneiform facet and of the facet for the medial cuneiform. The proximal (talar) articular margin is eroded laterally.

S4.1.2 Morphology

There are clear divisions of the cuneiform facets. There is no evidence of a naviculocuboid facet; the lateral side of the lateral cuneiform facet has a sharp edge with no rounding for a cuboid articulation.

S4.1.3. Paleopathology

The articular surfaces are smooth with only a slightly raised rounded edge to the dorsal and medial sides of the medial cuneiform facet.

S4.2 Cro-Magnon 4340 Right Navicular Bone (Feet B?)

S4.2.1 Preservation

The bone is largely complete (Fig. S5; Table S3). The margin of the talar facet is eroded in portions, especially medially, and the medial cuneiform facet and distal tuberosity are abraded. There is slight abrasion of the dorsal surface medially, with a 5 x 6 mm lacuna of cortical and trabecular bone on the dorsal tuberosity.

S4.2.2 Morphology

There are clear divisions of the cuneiform facets, with raised ridges on the dorsal halves of the medial to intermediate and intermediate to lateral facet divisions. There is a distinct naviculocuboid facet (Table S3), which rounds onto the lateral cuneiform articulation.

S4.2.2 Paleopathology

There are no degenerative alterations of the articular surfaces.

Table S3. Osteometrics of the Cro-Magnon 4339 and 4340 navicular bones, in millimeters.

	M#	***CM 4339***	***CM 4340***
Maximum thickness	8	17.3	(17.5)
Minimum thickness	7	8.2	10.1
Breadth	1	36.9	37.8
Height	2	26.4	30.9
Talar facet length	3	26.7	28.7
Talar facet breadth	4	21.5	22.0
Tuberosity projection[1]		7.0	7.5
Tuberosity proximodistal dimension[2]		16.8	(15.8)
Tuberosity dorsoplantar dimension[2]		13.6	12.8
Naviculocuboid facet height			6.7
Naviculocuboid facet breadth			6.4

[1] Maximum projection of the tuberosity from the talar articular surface.

[2] Maximum dimensions of the navicular tuberosity.

S4.3. Cro-Magnon 4341 Left Cuboid Bone (Feet A)

S4.3.1 Preservation

CM 4341 is a complete cuboid bone with peripheral damage or erosion (Fig. S6; Table S4). There is erosion to the dorsolateral distal corner, minor abrasion to the margins of

the metatarsal articular surface, and a patch of abrasion between the articular facets for the lateral cuneiform and navicular bones and the plantar surface.

S4.3.2 Morphology

The bone is notable for a well-defined facet for the navicular bone, separate from both the calcaneal facet and the one for the lateral cuneiform bone (Fig. S6). The lateral cuneiform facet is ovoid and flat.

Figure S6. The Cro-Magnon 4341 left cuboid bone, in dorsal (left), plantar (middle), lateral (upper right) and medial (lower right) views. Green arrow: navicular facet. Blue arrow: peroneus longus tendon surface.

The metatarsal 4 and 5 articular facets are clearly separated dorsally and plantarly, but blend across the middle of the combined surface. The metatarsal 4 one is largely flat; the metatarsal 5 one is distinctly concave dorsoplantarly and mediolaterally.

The bone exhibits a wide and shallow transverse plantar sulcus for the peroneus longus tendon (Fig. S6). Plantolaterally it exhibits a broad, 11 mm wide, smooth area for the tendon, extending halfway up the lateral side of the bone and apparently (given damage) to the edge of the calcaneal facet. It is not clear whether an os peroneum would have been present; however, in recent humans there is a continuum from a thickened tendon to small nodules within the tendon to the formation of a distinct sesamoid bone (Mittal et al., 2014), with an ossified os peroneum occurring in between ≈5% and ≈30% of individuals. It is nonetheless apparent that its presence cannot be inferred solely from the cuboid bone. There is one documented case of a Pleistocene human os peroneum, Dolní Věstonice 3, for which it was adherent to the cuboid in situ (Trinkaus and Jelínek, 1997).

S4.3.3 Paleopathology

The dorsal surface is distally irregular, with extra bone production similar to that from a periosteal reaction. There are several deep and small resorptive periarticular areas around the metatarsal articulations. There is an additional resorptive area, 4.5 mm in diameter and ≈3 mm deep, on the dorsal surface adjacent to the metatarsal 5 facet; the exposed trabeculae are rounded within the depression.

On the lateral surface, distodorsal of the peroneal tendon surface, there are two areas, deeper than broad, ≈1.5 mm in diameter, with exposed and rounded trabeculae. A third, similar area with remodeled trabeculae is located more distoplantar; it is less clear due to damage. There is a similar erosive area, 6 x 4 mm, dorsal of the navicular facet.

There are small osteophytic changes along small sections of the metatarsal facets' margins. The calcaneal facet, however, is smooth with no changes along its margin where intact.

Table S4. Osteometrics of the Cro-Magnon 4341 cuboid bone, in millimeters.

	M#			
Medial length	1	33.6	Lateral cuneiform facet height	10.7
Lateral length	2	22.9	Lateral cuneiform facet breadth	13.0
Calcaneal facet height		25.5	Metatarsal 4 facet height	22.1
Calcaneal facet breadth		24.5	Metatarsal 4-5 facets breadth	(24.5)
Navicular facet height		9.8	Metatarsal 4 facet breadth	12.0
Navicular facet breadth		8.1	Metatarsal 5 facet breadth	(14.0)

S4.4 Cro-Magnon 4342 Left Medial Cuneiform Bone (Feet A)

S4.4.1 Preservation

The bone (Fig. S7; Table S5) is intact with minor erosion of the medial and the plantomedial margins of the proximal (navicular) articular surface. There are minor areas of erosion of the distal (metatarsal) facet.

S4.4.2 Morphology

The bone exhibits a distinctly concave navicular facet. The metatarsal 1 facet is modestly convex plantarly and flat dorsally, with a torsion to the facet. The plantar half points directly distally, but the dorsal half points modestly medially.

The insertion areas for the tibialis anterior and peroneus longus tendons are evident but not marked.

S4.4.3 Paleopathology

There are no evident changes to the bone.

S4.5 Cro-Magnon 4344 Left Intermediate Cuneiform Bone (Feet A)

S4.5.1 Preservation

The bone (Fig. S7; Table S5) is dorsally largely intact and preserves most of the middle portion, but the plantar border is heavily broken and the lateral margin of its dorsal surface is eroded.

S4.5.2 Morphology and Paleopathology

There is little of note morphologically and no pathological changes to the preserved portions.

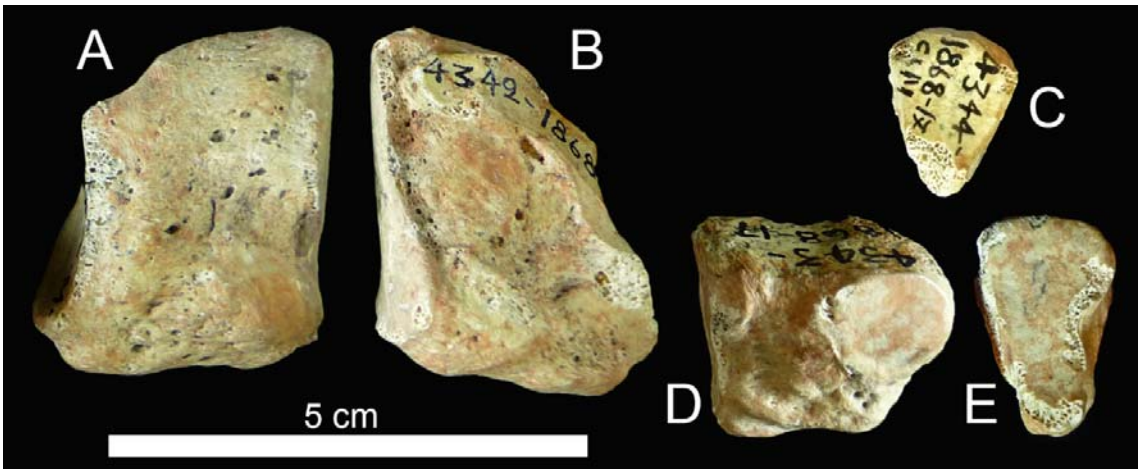

Figure S7. The Cro-Magnon 4342 left medial cuneiform bone in medial (A) and lateral (B) views. The Cro-Magnon 4344 left intermediate cuneiform bone is distal view (C). The Cro-Magnon 4343 left lateral cuneiform bone in lateral (D) and distal (E) views.

Table S5. Osteometrics of the Cro-Magnon 4342 to 4344 cuneiform bones, in millimeters.

	M# MC	***M# IC, LC***	***CM 4342***	***CM 4344***	***CM 4343***
Dorsal length	3	1	25.8	16.2	23.2
Middle length	2	2	23.5	14.8	19.9
Plantar length	1		27.6		
Proximal articular height	4		21.5	15.2	13.7
Proximal articular breadth		4	16.0	(17.0)	12.3
Distal articular height	5		30.8	--	20.4
Distal articular breadth		3	15.1	13.3	14.2
Total breadth[1]			19.3		
Cuboid facet height					12.2
Cuboid facet breadth					14.3
Tuberosity Height[2]					22.6
Tuberosity Length[2]					17.8
Tuberosity Breadth[2]					8.8

[1] Maximum mediolateral breadth across the musculoligamentous tuberosities.

[2] Dorsoplantar height of the bone, including the tuberosity, the proximodistal length of the tuberosity, and the mediolateral breadth of the tuberosity.

S4.6 Cro-Magnon 4343 Left Lateral Cuneiform Bone (Feet A)

S4.6.1 Preservation

The bone (Fig. S7; Table S5) is complete, but most of its medial surface and the medial margin of the dorsal surface are abraded. The proximal articular surface is eroded

medially and plantarly, and the margins of metatarsal facet are eroded. The plantar border is intact with the tuberosity, with erosion to the distal tuberosity.

S4.6.2 Morphology and Paleopathology

There is little of note on the bone, except that the plantar tuberosity is small and projects little beyond the distal (metatarsal 3) facet. There are no alterations to the articular surfaces.

S5: The Cro-Magnon Metatarsal Bones

S5.1 Cro-Magnon 4345 Left Metatarsal 1 (Feet A)

S5.1.1 Preservation

The bone (Fig. S8; Table S6) is largely complete, although the lateral half to two-thirds of the base and a significant portion of the proximal half of the lateral surface of the diaphysis are missing. The absent portions are filled with plaster and wax, which has been removed virtually to permit the virtual reassembly of Feet A (Figs. 1, S15 and S16). The plantar extensions of the head are also heavily abraded.

S5.1.2 Morphology

There is minimal concavity to the preserved medial portion of the base. Distally there are large dorsal tubercles by the head, especially laterally. The intersesamoid crest is not sufficiently preserved to indicate the lateral deviation usually associated with a normal hallucal orientation.

S5.1.3 Paleopathology

There are no lesions on the bone.

Figure S8. Medial view of the CM 4345 left metatarsal 1 (A), lateral view of the CM 4545bis right metatarsal 1 (B), and medial view of CM 4345bis (C).

S5.2 Cro-Magnon 4345bis Right Metatarsal 1 (Feet B)

S5.2.1 Preservation

The metatarsal (Fig. S8; Table S6) is largely complete but with bone loss to corners of the base and head. The base has lost bone in dorsal and plantar patches of the medial side and dorsally on the lateral side. The medial surface and two-thirds of the dorsal surface of the

head are missing, the dorsal portion of the lateral surface of the head is abraded, and distally there are two areas with loss of the articular surface. The diaphysis is intact.

S5.2.2 Morphology

The medial cuneiform facet is distinctly transversely concave, but without a dorsoplantar torsion. The lateral base is sufficiently intact to indicate the absence of a metatarsal 2 facet. The peroneal tubercle is a minimally projecting three-quarters of a circle along the margin of the proximal facet, 8.6 mm high and 8.7 mm wide. The intersesamoid crest deviates laterally, as in normal hallucal orientation.

S.5.2.3 Paleopathology

There is slight new bone deposition along the lateral border of the dorsal surface of the shaft. A slight plantar resorptive area (6 mm wide and 5 mm proximodistal), not clearly circumscribed, is in contact with the plantar head. There are no changes to the articular surfaces.

S5.3 Cro-Magnon 4346 Right Metatarsal 2 (Feet B?)

S5.3.1 Preservation

The bone is complete (Fig. S9; Table S6), with minor erosion of the margins of the base and the medial and lateral tubercles of the head. The medial and lateroplantar head are missing bone, as are the distal dorsal tubercles. The diaphysis is intact.

S5.3.2 Morphology

The medial base has one very small facet for the medial cuneiform bone, and then an irregular area distal of that facet. There is no evidence of a metatarsal 1 facet. There are (or were) dorsal and plantar metatarsal 3 facets, but the plantar one is mostly eroded away. The shaft is straight, and there are no marks for the dorsal interosseus muscles.

Figure S9. Lateral view of the CM 4346 right metatarsal 2 (left) and medial view of CM 4346 (right).

S5.3.3 Paleopathology

The articular surfaces show no degeneration. Although the shaft appears normal, there is a longitudinal sulcus along the lateroplantar diaphysis. In the proximodistal middle of the sulcus, there is a small swelling of bone with very small perforating foramina, as though a small blood vessel along the sulcus was bridged (Fig. S9). Its significance is unclear and not necessarily pathological.

Table S6. Osteometrics of the Cro-Magnon 4345 to 4346 metatarsal 1 and 2 bones, in millimeters and degrees.

	M#	***CM 4345***	***CM 4345bis***	***CM 4346***
Maximum length	1, 2	66.6	65.1	77.4
Articular length	1b	65.2	62.9	74.0
Shaft height	4	14.3	14.5	9.8
Shaft breadth	3	11.6	13.1	8.7
Shaft circumference		41.0	43.0	29.0
Proximal maximum height	7	--	--	20.6
Proximal maximum breadth	6	--	17.8	10.4
Proximal articular height	7b	--	--	(19.0)
Proximal articular breadth	6b	--	14.8	12.3
Distal height	9	(21.0)	--	14.8
Dorsal articular breadth	8	20.0	--	
Distal maximum breadth	8a			(11.0)
Distal articular breadth	9			10.0
Horizontal head angle		--	8°	
Horizontal base angle				74°
Vertical base angle				79°
MT 1-2 facet presence		--	abs	abs

S5.4 Cro-Magnon 4347 Right Metatarsal 4 (Feet B)

S5.4.1 Preservation

The bone (Fig. S10; Table S7) is largely complete with minor erosion to the margins of the cuboid and metatarsal facets. The medial plantar articular extension of the head is abraded, and all of the lateral surface of the head is absent.

S5.4.2 Morphology

There is little of note morphologically on the bone. It does exhibit strong torsion, indicating a well formed transverse pedal arch.

S5.4.3 Paleopathology

On the medial surface of the shaft, 6 mm distal of the metatarsal 3 facet, there are two round well-circumscribed depressions (each 2 mm in diameter), one dorsal and slightly proximal of the other. The plantar one has a small bone formation within it, the other one is relatively smooth.

The head presents two areas (Fig. S10C). The areas are separated by a sagittal sulcus plantarly. The medial half, including the medial articular extension, has a normal unaltered articular surface. The lateral half is more proximal relative to the medial one. Its surface is irregular (or granular) with a few small foramina.

Figure S10. Medial (A) and lateral (B) views of the Cro-Magnon 4347 (on the right) and 4348 (on the left) fourth metatarsals, with a distal view of the CM 4347 right metatarsal 4.

S5.5 Cro-Magnon 4348 Left Metatarsal 4 (Feet B)

S5.5.1 Preservation

The bone is complete (Fig. S10, Table S7) with minor abrasion, especially to the lateral head and its plantar extension.

S5.5.2 Morphology

The dorsal tubercles for the head are well developed. It exhibits a torsion similar to CM 4347.

S5.5.3 Paleopathology

There may be a slight remodeling of the lateral head dorsal tubercle, but the head articular surface exhibits none of the remodeling seen on CM 4347.

S5.6 Cro-Magnon 4349 Right Metatarsal 5 Right (Feet B)

S5.6.1 Preservation

The bone is complete (Fig. S11, Table S7), with minor bone loss to the dorsal head and slight abrasion to the dorsal base.

S5.6.2 Morphology

There are no features of note.

S5.6.3 Paleopathology

The head displays pathological alterations of the whole articular surface (Fig. S11D). There are at least a dozen small foramina or openings, including a slightly larger pair in a distal depression with remodeled trabeculae. The head appears to have turned laterally. None of the original articular surface is unaltered.

Figure S11. Plantar (A) and lateral (B) views of the Cro-Magnon 4349 metatarsal 5, and plantar view (C) of the CM 4350 metatarsal 5, plus a distal view of the pathological CM 4349 metatarsal 5 head.

S5.7 Cro-Magnon 4350 Left Metatarsal 5 (Feet C?)

S5.7.1 Preservation

The bone preserves its proximal half to two-thirds (Fig. S11C, Table S7). The margins of the cuboid articular surface are eroded, especially lateroplantarly. The plantar half of the styloid process is absent. The diaphyseal cortical bone is abraded plantarly.

S5.7.2 Morphology and Paleopathology

There are no features of note. There are no alterations of the proximal articulations.

S6: The Cro-Magnon Pedal Phalanx

S6.1 Cro-Magnon 4351 Proximal Phalanx 1 (Feet B?)

S6.1.1 Preservation and Side Assessment

The bone (Fig. S12; Table S8) is complete with minor erosion to the plantar proximal articulation. The plantar surfaces of the head plantar articular extensions are absent.

Based on an assumed lateral deviation for a proximal pedal phalanx given normal hallucal orientation, the right deviation of the head in dorsal view it would make it a right phalanx. Yet, the orientation of the base relative to the diaphysis, and assuming normal hallucal lateral deviation, would suggest a left phalanx. Given uncertainty in the degree to which the distal articulation is pathologically altered (see below), the indication from the base should probably be given priority.

Table S7. Osteometrics of the Cro-Magnon 4347 and 4348 metatarsal 4s and the CM 4349 and 4350 metatarsal 5s, in millimeters and degrees. "Path" indicates a pathologically altered dimension.

	M#	*CM 4347*	*CM 4348*	*CM 4349*	*CM 4350*
Maximum length	2	74.2	73.9	70.3	--
Articular length	1b	71.0	72.0	64.0	--
Shaft height	4	11.5	11.2	7.8	8.6
Shaft breadth	3	7.3	7.6	11.5	10.0
Shaft circumference		33.0	33.5	31.5	30.0
Proximal maximum height	7	18.8	20.2	14.6	14.3
Prox. max. breadth re cuboid[1]	6b	14.9	15.1	20.3	18.8
Prox. max. breadth re MT4[1]				20.6	19.4
Prox. articular height	7b	18.3	18.1	14.5	13.4
Prox. articular breadth re cuboid[1]		12.3	11.0	14.6	14.7
Distal height	9	18.0	16.0	15.1 path	--
Distal maximum breadth	8a	11.4	11.6	12.7 path	--
Distal articular breadth	8	(10.5)	10.5	--	--
Horizontal base angle		68°	71°	54°	55°
Vertical base angle		75°	79°		
Metatarsal 3 facet height		8.7	9.6		
Metatarsal 3 facet breadth		14.0	18.3		
Metatarsal 4 facet height				10.0	10.0
Metatarsal 4 facet breadth				15.0	12.7
Metatarsal 5 facet height		14.1	12.9		
Metatarsal 5 facet breadth		13.5	12.6		

[1] The breadths of the proximal (cuboid) portion parallel to the cuboid facet or perpendicular to the metatarsal (MT) 4 facet.

S6.1.2 Morphology

There is one foramen in the proximal articular surface. There is a small tuberosity, proximally, on the dorsal and slightly lateral surface of the diaphysis, close to the base, for the extensor hallucis brevis tendon.

S6.1.3 Paleopathology

All of the articular surface of the head is irregular and bumpy (Figs. S12C and S12D), but it maintained its normal overall configuration. There is an area 1.5 mm in diameter on the medial plantar extension of the head. A large foramen is present in the mid-distal surface. The head extends proximally on the mid-dorsal margin, and the medial side of the head appears to project medially. Overall it appears as a degeneration of the articular surface, but without associated osteophytes (see discussion in text).

Plantarly there is a hollow area, 7 x 6 mm, between the plantar head extensions, which may be resorptive but is largely formed by the plantar and proximal extensions of the plantar head surface.

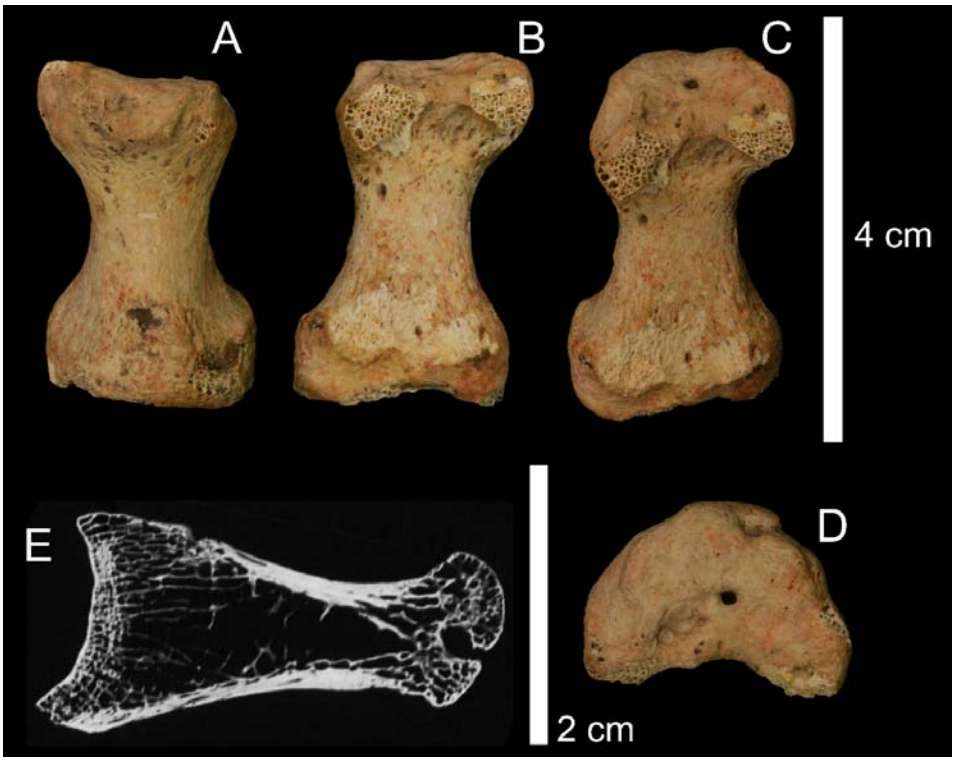

Figure S12. Dorsal (A) and plantar (B) views of the Cro-Magnon 4351 proximal pedal phalanx 1, with distoplantar (C) and distal (D) views of the pathological head. The mid-sagittal CT slice (E) reveals a subchondral cyst connected to the mid-distal foramen.

Table S8. Osteometrics of the Cro-Magnon 4351 proximal pedal phalanx, in millimeters. "Path" indicates measurements affected or possibly affected by the pathological alterations of the head.

	M#	
Maximum length	1	33.8
Articular length	1a	(30.5) path
Shaft height	3	9.1
Shaft breadth	2	11.5
Shaft circumference		33.0
Proximal maximum height	2a	17.3
Proximal maximum breadth	2a	20.9
Proximal articular height		14.5
Proximal articular breadth		19.5
Distal height	3b	(13.4) path
Distal maximum breadth	2b	(18.9) path

S7: Associations of the Cro-Magnon Pedal Remains

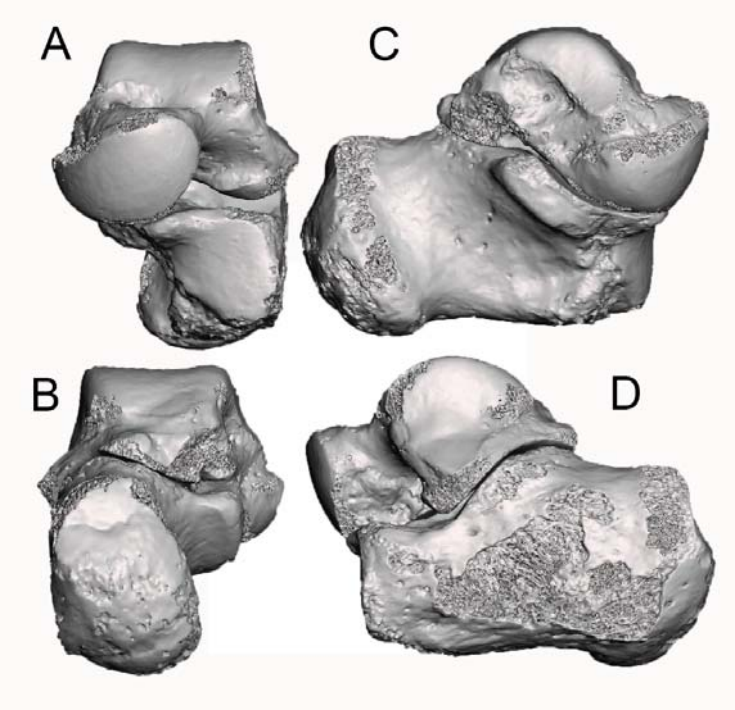

Figure S13. Virtual mirror imaging of the CM 4336 right calcaneus and its articulation with the CM 4337 left talus, in anterior (A), posterior (B), medial (C) and lateral (D) views.

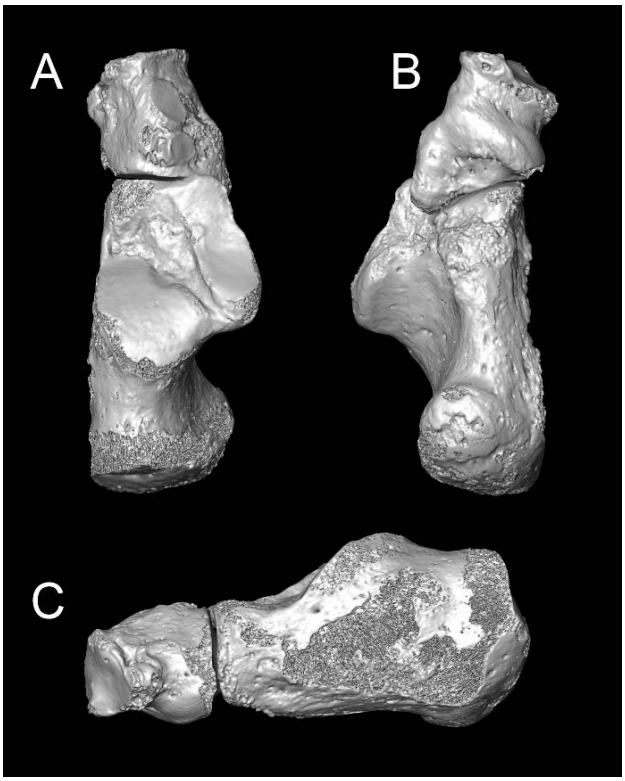

Figure S14. Virtual mirror imaging of the CM 4336 right calcaneus and its articulation with the CM 4341 left cuboid bone, in dorsal (A), plantar (B) and lateral (C) views.

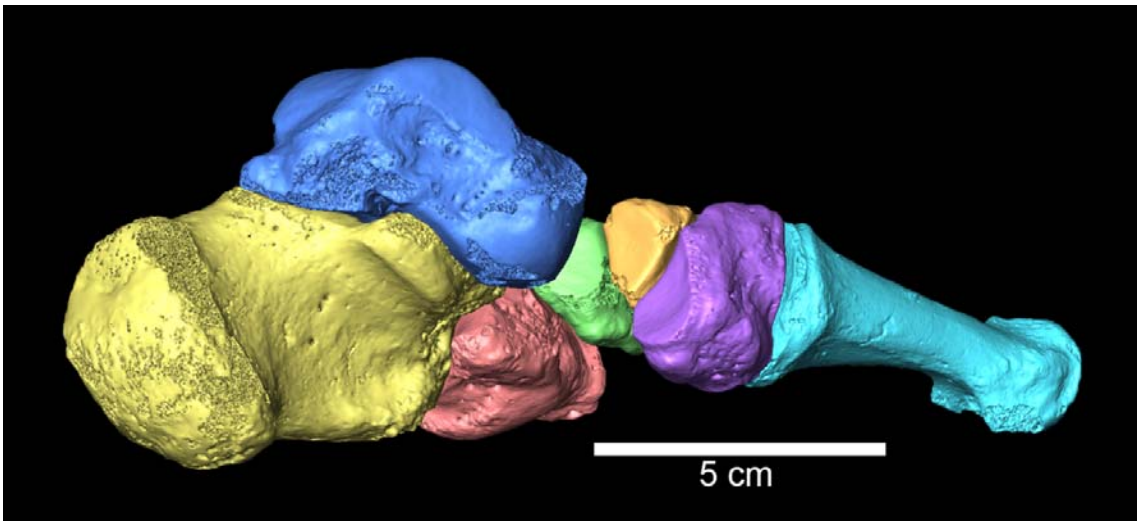

Figure S15. Virtual articulation of the Cro-Magnon Feet A in posteromedial view, with the CM 4337 talus, CM 4336 calcaneus, CM 4341 cuboid bone, CM 4342 to 4344 cuneiform bones, and CM 4345 metatarsal 1. It shows, in particular, the talocalcaneal, anterior tarsal, and tarsometatarsal 1 articulations.

Table S9. Predictions of tarsal, metatarsal and proximal phalanx dimensions from single or combined metatarsal articular lengths, using simple or multiple linear regression as appropriate. Navicular predictions from Libben Native American sample. Other predictions from the pooled Native American, Euroamerican, Afroamerican, and European samples. Data from Trinkaus (1975a) and Pablos et al. (2017).

Predictor(s)			Prediction				
		Artic. length		Mean ± SE	95% CI	r^2	n
MT-1 MT-4 MT-5	CM 4345bis CM 4347 CM 4349	62.9 71.0 64.0	Talus length	53.6 ± 3.0	47.8 – 59.4	0.414	215
MT-1	CM 4345	65.2	Talus length	55.0 ± 3.0	49.0 – 61.0	0.582	224
MT-1	CM 4345bis	62.9	Talus length	53.7 ± 3.0	47.7 – 59.7	0.408	215
MT-1 MT-4 MT-5	CM 4345bis CM 4347 CM 4349	62.9 71.0 64.0	Navicular talar length	28.2 ± 1.6	25.0 – 31.4	0.418	40
MT-1 MT-4 MT-5	CM 4345bis CM 4347 CM 4349	62.9 71.0 64.0	Navicular talar breadth	21.1 ± 1.2	18.7 – 23.5	0.401	40

Table 9 (cont.)

Predictor(s)			Prediction				
		Artic. length		Mean ± SE	95% CI	r^2	n
MT-1	CM 4345	65.2	MT-2	77.8 ± 2.4	73.2 – 82.5	0.791	233
MT-1	CM 4345bis	62.9	MT-2	75.4 ± 2.4	70.7 – 80.1	0.791	233
MT-4 MT-5	CM 4347 CM 4349	71.0 64.0	MT-1	62.6 ± 2.4	57.9 – 67.3	0.687	224
MT-4 MT-5	CM 4347 CM 4349	71.0 64.0	MT-2	75.8 ± 2.0	71.9 – 79.5	0.849	224
MT-1	CM 4345	65.2	PP-1	31.8 ± 1.7	28.3 – 35.2	0.556	231
MT-1	CM 4345bis	62.9	PP-1	30.7 ± 1.7	27.3 – 34.1	0.556	231

Table S10. Estimated femoral head diameters from acetabular height (AH) and femoral head diameters (FHD) for the Cro-Magnon coxal bones and femora attributed to the three appendicular individuals, Alpha to Gamma, in millimeters. Data from Thibeault and Villotte (2018: Tables 2 and 4). For Beta and Gamma, the femoral measurements are employed; for Alpha the average of the values estimated from the two acetabulae is used.

Alpha		***Beta***		***Gamma***	
CM 4314a	46.7 (AH)	CM 4317	42.9 (AH)	CM 4315	50.0 (AH)
CM 4314b	48.6 (AH)	CM 4321	42.2 (FHD)	CM 4318	49.8 (AH)
				CM 4322	49.4 (FHD)
Value Used	47.7		42.2		49.4

Table S11. Prediction of the geometric mean of the talar trochlear length and breadth (TRC) from femur head diameter (FHD), based on a pooled sample of recent Native Americans and Late Pleistocene humans. The femoral head diameters are the values used for each appendicular individual in Table S10.

Predictor (FHD)		***Target (TRC)***		***Prediction (TRC)***			
				Mean ± SE	95% CI	r^2	n
Alpha	47.7			31.7 ± 1.7	28.3 – 35.1	0.569	67
Beta	42.6	CM 4338	28.5	28.9 ± 1.7	25.5 – 32.4	0.569	67
Gamma	49.7	CM 4337	33.4	32.8 ± 1.7	29.3 – 36.2	0.569	67

Table S12. The likelihoods of pedal remains being associated with one of the designated Cro-Magnon feet. Following Thibeault and Villotte (2018), they are categorized in terms of: impossible, unlikely, possible, probable, secure. The bones that make up the articulating cores of Feet A and B are labeled as "secure," and therefore by default they are unavailable for the other feet.

Number	***Bone***	***Side***	***Feet A***	***Feet B***	***Feet C***
4337	Talus	left	secure	--	--
4338	Talus	right	impossible	unlikely	probable[1]
4336	Calcaneus	right	secure	--	--
4339	Navicular	right	impossible	unlikely	probable[1]
4340	Navicular	right	impossible	possible	impossible
4341	Cuboid	left	secure	--	--
4342	Med. Cuneiform	left	secure	--	--
4344	Int. Cuneiform	left	secure	--	--
4343	Lat. Cuneiform	left	secure	--	--
4345	Metatarsal 1	left	secure	--	--
4345bis	Metatarsal 1	right	possible	probable	unlikely
4346	Metatarsal 2	right	possible	probable	unlikely
4347	Metatarsal 4	right	--	secure	--
4348	Metatarsal 4	left	--	secure	--
4349	Metatarsal 5	right	--	secure	--
4350	Metatarsal 5	left	impossible	unlikely	possible
4351	Prox. Phalanx 1	--	possible	probable	possible[2]

[1] The CM 4338 and CM 4339 tarsals form a secure articulating pair. They are designated "probable" for Feet C only because they could derive from Feet B, however unlikely that is based on size.

[2] Given the smaller size of the Feet C elements and the close fit of CM 4351 to either Feet A or B, it is less likely that CM 4351 derives from Feet C. However, it is nonetheless possible that it does.

S8: Tarsometatarsal Lengths of Cro-Magnon Feet A

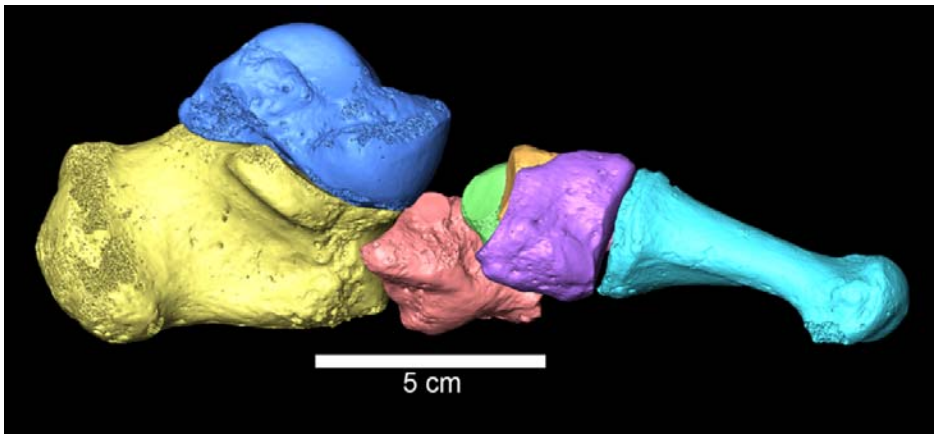

Figure S16. Medial view of the virtually assembled bones of the Feet A left tarsometatarsal skeleton. The distance between the talus and the cuneiform bones is estimated, based on the similarly sized CM 4340 navicular bone, which nonetheless does not articulate properly with the talus or the cuneiform bones. The medial longitudinal arch is too low as articulated, since placing the bones in maximum articular congruence tends to produce a highly pronated foot. The original habitual arch height is unknown, and unknowable [contra Pruner-Bey (1865-75: 84)]. In any case, arch height varies with foot posture and stance phase, and across individuals irrespective of footwear (Arulsingh et al., 2015; D'Août et al., 2009; Martin, 2011).

Table S13. Tarsometatarsal lengths of the Cro-Magnon Feet A (Gamma) pedal skeleton, and available Late Pleistocene measurements and recent human summary data, in millimeters.

	Tarsometatarsal (TMT) Length[2]	Anterior TMT Length[3]	Posterior TMT Length[3]	Femur Bicondylar Length
Cro-Magnon Feet A	190	131	59	(475.5)[4]
E/MUP[1]				
Caviglione 1	187.5	140	47.5	469.5
Dolní Věstonice 15[5]	165	116	49	--
Dolní Věstonice 16	180	120	60	467.5
Pavlov 37	200	146.5	53.5	--
Pavlov 38	174.5	121	53.5	--
Předmostí 3	192	135.5	56.5	486.5
Sunghir 1	183	133	50	498
MPMH[1]				
Qafzeh 8	174	119	55	(507)
Qafzeh 9	162	120	42	469.5
Skhul 4	182	118	64	490
Neandertals				
La Ferrassie 1	182	126	56	(458)
La Ferrassie 2	150	104	46	407
Kiik-Koba 1	181	123	58	--
Shanidar 1	185	127	58	(458)
Tabun 1	159	113	46	410

Table S13 (cont.)

Recent Humans				
Native Americans[6]	165.2 ± 9.3	119.1 ± 7.0	46.1 ± 3.6	452.2 ± 24.4
Northeast Africans[7]	165.1 ± 12.2	115.5 ± 9.1	49.6 ± 4.8	433.4 ± 28.1

[1] E/MUP: Early and Mid Upper Paleolithic modern humans. MPMH: Middle Paleolithic modern humans.
[2] Tarsometatarsal (TMT) length: proximal calcaneal tuberosity to the distal MT-1 head, measured parallel to the plantar plane of the articulated TMT skeleton.
[3] The distances, parallel to the plantar plane, from the proximal calcaneal tuberosity to the mid talar trochlea (posterior) and mid talar trochlea to the distal MT-1 head (anterior).
[4] The femur bicondylar length for Feet A is based on the CM 4322 femur, the more complete one in the Gamma lower limb bones (Thibeault and Villotte, 2018).
[5] The Dolní Věstonice 15 TMT skeleton is included despite the abnormalities of his skeleton. The lower limbs distal of the femora appear normal despite their small size, including the proportions of his pedal remains (Trinkaus et al., 2006).
[6] Libben Woodland sample, Ohio, USA; TMT n = 40, femur n = 16.
[7] Keneh pre-dynastic Egyptian sample; TMT n= 25, femur n = 24

Table S14. Stature predictions from Cro-Magnon pedal remains, in centimeters.

Bone(s)	Length	Feet A	Feet B	Feet C	Ref. Sample[1]	Ref.[2]
Talus	maximum	175.6		166.9	AfrAm-F	1
Calcaneus	maximum	175.2			AfrAm-M	1
MT-1	maximum	172.7	170.6		pooled	1
MT-2	maximum		174.4		EurAm-F	1
Calc+MT-1	maximum	172.6			pooled	1
Tal+MT-1	maximum	174.3			pooled-F	1
MT-1	articular	174.2	172.4		Eur-M	2
MT-2	articular		173.0		Eur-M	2
MT-1	articular	172.9	169.1		pooled	3
MT-2	articular		166.7		pooled	3
MT-4	articular		171.6		pooled	3

[1] Afr-Am: African-Americans; Eur-Am: European Americans; pooled: AfrAm + EurAm; Eur: Coimbra Portuguese; F: females; M: males.
[2] 1: Pablos et al., 2013; 2: Cordeiro et al., 2009; 3: Byers et al., 1989.

S9: Comparative Samples

Table S15. Recent human comparative samples.

	Site/Collection	Location	Reference
Native American	Libben	Ohio, USA	Trinkaus, 1975a
Euroamerican	Hamann-Todd	Ohio, USA	Pablos et al., 2017
Afroamerican	Hamann-Todd	Ohio, USA	Pablos et al., 2017
Northeast African	Keneh	Egypt	Rhoads and Trinkaus, 1977
Medieval Europe	San Pablo	Spain	Pablos et al., 2017
Medieval Europe	Mistihalj	Serbia	Rhoads and Trinkaus, 1977

Table S16. Late Pleistocene specimens included in the comparative samples.

Neandertals:

Amud 1 and 9, La Chapelle-aux-Saints 1, La Ferrassie 1 and 2, Jarama VI 1, Kiik-Koba 1, Krapina 218, 219, 235 to 240.1, 243 to 246.2, La Quina 1, Palomas 92, Petit-Puymoyen 7, Regourdou 1 and 2, Shanidar 1, 3, 4, 5, 6 and 8, Spy 1 and 2, Tabun 1

Middle Paleolithic modern humans:

Qafzeh 3, 8 and 9, Skhul 4, 5, 6 and 7

Early/Mid Upper Paleolithic humans:

Barma Grande 1 and 2, Baousso da Torre 2, Caviglione 1, Dolní Věstonice 3, 13 to 16, 54 and 55, Grotte des Enfants 4 to 6, Mladeč 30, Nahal Ein Gev 1, Ostuni 1, Paglicci 25, Pataud 1, Paviland 1, Pavlov 37 and 38, Předmosti 3, 4, 9, 10 and 14, Sunghir 1 to 3, Veneri 1 and 2

Late Upper Paleolithic humans:

Arancio 1, Arene Candide 2, 4, 5, 10 and 13, Bichon 1, Cap Blanc 1, Chancelade 1, Continenza 1, Ein Gev 1, Neve David 1, Lafaye 1, Laugerie Basse 4, La Madeleine 1, Maritza 2, El Mirón 1, Oberkassel 1, Oetrange 1, Ohalo 2, Le Peyrat 5, San Teodoro 1 and 4, Tagliente 1

S10: Proposed Cro-Magnon Associations

Table S17. Proposed associations of the Cro-Magnon adult remains, based on those proposed for the lower limbs by Thibeault and Villotte (2018), for the upper limbs by Villotte et al. (2020), for the cranial and mandibular remains by Trinkaus et al. (2021) and for the pedal remains by Thibeault and Villotte (2018) and here. The individuals (Alpha to Delta) are those based on the appendicular remains, restricting the traditional Cro-Magnon 1 to 4 designations to the crania and the one directly associated mandible.[1]

	Alpha	Beta	Gamma	Delta[3]
Neurocranium	4253 (#1)	4255 (#3) or 4259 (#4)[2]		4254 (#2)
Maxilla/Mandible	4253 (#1)	4256 or 4257/4258[2]		4254 (#2)
Clavicle	4290			
Scapula	4292			
Humerus		4294,4295	4293	
Ulna	4299	4301	4300,4302	4297,4298
Radius	4304	4305	4303	
Coxal bone	4314a,4314b	4316a,4317,4316b?	4315,4318	
Sacrum		4314c	4319?	
Femur	4323,4327,4325	4321,4324,4329	4322,4323,4328	
Tibia	4331,4332		4330,4333	
Fibula	4335		4334	
Talus		4338	4337	
Calcaneus			4336	
Navicular[4]	4340?	4349		
Cuboid			4341	
Cuneiforms			4342,4343,4344	
Metatarsal 1	4345bis		4345	
Metatarsal 2	4346			
Metatarsal 4	4347,4348			
Metatarsal 5[4]	4349	4350?		
Prox. Phalanx 1	4351			

[1] A number of the arm remains and the few hand remains cannot be reliably assigned to one of these individuals (Villotte et al. (2020). They are therefore not included here.

[2] As discussed in Trinkaus et al. (2021), the CM 4256 mandible and the CM 4257/4258 maxilla/mandible likely derive from the Beta and Gamma postcranial pair as well as from the CM 4255 and CM 4259 cranial pair. It is not currently possible to determine which way these three pairs might be associated.

[3] As discussed in Trinkaus et al. (2021), the association of CM 4254 cranium (Cro-Magnon 2) with Delta is largely based on its unlikely association with Beta or Gamma, and the assumption of only four adults in the Cro-Magnon sample.

[4] As discussed in the text, the CM 4340 navicular bone and the CM 4350 metatarsal 5 are attributed to Gamma and Beta respectively in part on size and in part due to non-congruence with the same or adjacent bones in each of the other two sets of pedal remains. It is possible, if less likely given the absence of a fourth individual in the pelvic and leg remains, that they derive from a fourth individual.

S11: Supporting Information References

Arulsingh, K., Pai, G., Samuel, A.J., 2015. Does medial arch height differ from barefoot runners to shod runners? – An analytical study. Ind. J. Physiother. Occup. Therapy 9, 159-165. http://doi 1 0.5958/0973-5674.2015.00032.5.

Bräuer, G., 1988. Osteometrie. in: Knussman, R. (Ed.) Anthropologie I. Fischer, Stuttgart. pp. 160-232.

Byers, S., Akoshima, K., Curran, B., 1989. Determination of adult stature from metatarsal length. Am. J. Phys. Anthropol. 79, 275-279. https://doi.org/10.1002/ajpa.1330790303

Cordeiro, C., Muñoz-Barús, J.I., Wasterlain, S., Cunha, E., Vieira, D.N., 2009. Predicting adult stature from metatarsal length in a Portuguese population. Forensic Sci. Intl. 193, 131.e1-131.e4. https://doi.org/10.1016/j.forsciint.2009.09.017.

D'Août, K., Pataky, T.C., De Clerq, D., Aerts, P., 2009. The effects of habitual footwear use: foot shape and function in native barefoot walkers. Footwear Sci. 1, 81-94. http:// doi.10.1080/19424280903386411.

Martin, R.L., 2011. The ankle and foot complex. in: Levangie, P.K., Norkin, C.C. (Eds.), Joint Structure and Function 5th ed. F.A. Davis, Philadelphia, pp. 440-481.

Matiegka J. 1938. Homo předmostensis. Fosilní člověk z Předmostí na Moravě II. Ostatní Části Kostrové. Česká Akademie Věd a Umění, Prague.

Mittal, P.S., Joshi, S.S., Chhaparwal, R., Joshi, S.D., 2014. Prevalence and morphometry of os peroneum amongst central Indians. J. Clin. Diagn. Res. 8, AC08-AC10. https://doi:10.7860/JCDR/2014/10452.5079.

Morimoto, I., 1960. The influence of squatting posture on the calcaneus in the Japanese. Formation of the forward extension complex of the posterior talar articular surface. J. Anthropol. Soc. Nippon 68, 16-22. https://doi.org/10.1537/ase1911.68.16.

Pablos, A., Gómez-Olivencia, A., Garcia-Pérez, A., Martínez, I., Lorenzo, C., Arsuage, J.L., 2013. From toe to head: Use of robust regression methods in stature estimation based on foot remains. Forensic Sci. Intl. 296, 229.e1-299.e7. https://doi.org/10.1016/j.forsciint.2013.01.009.

Pablos, A., Pantoja-Pérez, A., Martínez, I., Lorenzo, C., Arsuaga, J.L. (2017) Metric and morphological analysis of the foot in the Middle Pleistocene sample of Sima de los Huesos (Sierra de Atapuerca, Burgos, Spain). Quatern. Intl. 433, 103-113. https://dx.doi.org/10.1016/j.quaint.2015.08.044.

Rhoads, J.G., Trinkaus, E., 1977. Morphometrics of the Neandertal talus. Am. J. Phys. Anthropol. 46, 29-44. https://doi/10.1002/ajpa.1330460106 .

Sewell, R. B. S., 1904-05. A study of the astragalus. J. Anat. Physiol. 38, 233-247, 423-434; 39, 74-88.

Thibeault, A., Villotte, S., 2018. Disentangling Cro-Magnon: A multiproxy approach to reassociate lower limb skeletal remains and to determine the biological profiles of the adult individuals. J. Archaeol. Sci. Rep. 21, 76-86. https://doi.10.1016/j.jasrep.2018.06.038.

Trinkaus, E., 1975a. A Functional Analysis of the Neandertal Foot. PhD. Thesis, University of Pennsylvania.

Trinkaus, E., 1975b. Squatting among the Neandertals: A problem in the behavioral interpretation of skeletal morphology. J. Archaeol. Sci. 2, 327-351. https://doi.org/10.1016/0305-4403(75)90005-9.

Trinkaus, E., Jelínek, J., 1997. Human remains from the Moravian Gravettian: The Dolní Věstonice 3 postcrania. J. Hum. Evol. 33, 33-82. https://doi.org/10.1006/jhev.1997.0142.

Trinkaus, E., Hillson, S.W., Franciscus, R.G., Holliday, T.W., 2006. Skeletal and dental paleopathology. in Trinkaus, E., Svoboda, J.A. (Eds) Early Modern Human Evolution in Central Europe: The People of Dolní Věstonice and Pavlov. Oxford University Press, New York. pp. 419-458.

Trinkaus, E., Buzhilova, A.P., Mednikova, M.B., Dobrovolskaya, M.V., 2014. The People of Sunghir: Burials, Bodies and Behavior in the Earlier Upper Paleolithic. Oxford University Press, New York.

Trinkaus, E., Wojtal, P., Wilczyński, J., Sázelová, S., Svoboda, J., 2017. Palmar, patellar and pedal human remains from Pavlov. PaleoAnthropology 2017, 73-101. https://doi.10.4207/pa.2017.art106 .

Trinkaus, E., Lacy, S.A., Thibeault, A., Villotte, S., (2021) Disentangling Cro-Magnon: The dental and alveolar remains. J. Archaeol. Sci. Rep. 37, 102991. https://doi.org/10.1016/j.jasrep.2021.102911.

Villotte, S., Samsel, M., Sparacello, V., 2017. The paleobiology of two adult skeletons from Baousso da Torre (Bausu da Ture) (Liguria, Italy): Implications for Gravettian lifestyle. C. R. Palevol 16, 462–473. https://doi.org/10.1016/j.crpv.2016.09.004.

Villotte, S., Thibeault, A., Sparacello, V., Trinkaus, E., 2020. Disentangling Cro-Magnon: The adult upper limb skeleton. J. Archaeol. Sci. Rep.33, 102475. https://doi.org/10.1016/j.jasrep.2020.102475.